Spectroscopic Analysis of Various Phases of Water with an Intrinsic Near-Infrared Optical Sensor System

Osazonamen J. Igbinosun

A thesis

submitted in partial fulfillment of the

requirements for the degree of

Master of Science

University of Washington

2013

Committee:

Stephen Wood

Evan Abramson

Adam Bruckner

Program Authorized to Offer Degree:
Earth and Space Sciences

University of Washington

Abstract

Spectroscopic Analysis of Various Phases of Water with an
Intrinsic Near-Infrared Optical Sensor System

Osazonamen J. Igbinosun

Chair of the Supervisory Committee:
Professor Stephen E. Wood
Earth and Space Sciences

Results and analysis are reported for near-infrared spectra obtained using an intrinsic optical sensor system. An experimental facility was designed to integrate fiber optic cables with an FTIR spectrometer. Wavelength-dependent spectral signatures were observed for the solid, liquid, and adsorbed phases of water at λ =1.94 and λ =1.45 μm. The data obtained can be used to characterize the water abundance of a medium on very small scales and can aid our understanding of the behavior of water and thermal properties of planetary surfaces by observing, for example, ice formation in void spaces between mineral grains. This system will be further developed for use in an environmental simulation facility to analyze Mars analog soils. The implications of this work could impact future space missions in regard to the availability of critical resources for human missions and the search for non-terrestrial life.

TABLE OF CONTENTS

Page

LIST OF FIGURES

LIST OF TABLES

Acknowledgements

The author wishes to express thanks to Stephen E. Wood, Evan Abramson, Adam Bruckner, Allen Hart, Michael McCarthy, Robert Holzworth, Alan Gillespie, Loren Kruse, the Department of Earth and Space Sciences, the Graduate Opportunities and Minority Achievement Program of the University of Washington, the National Science Foundation, and the University of Washington Astrobiology Program.

Ch. 1 Introduction

Significance of subsurface water on Mars

Studies of the subsurface of Mars can uncover fundamental properties of the regolith that can aid in understanding the present-day and past environment. Research in this area can also uncover clues as to whether the subsurface is hospitable to microbial life. Lastly, as the field of human exploration seeks to venture to other celestial bodies (including the planet Mars) studies of the subsurface, in particular, investigations of water in the subsurface, could provide key insight into the utilization of planetary resources.

The presence of ice within the pore space of planetary regolith can significantly affect its thermal properties, especially on planets with thin or absent atmospheres. Thermal conductivity, the measure of a material's ability to conduct heat, is sensitive to soil particle contact points and the void spaces created between them—especially when ice is present, even in small quantities. Theoretical models predict that an ice volume fraction of as little as 0.1% can increase the thermal conductivity of Martian soil by a factor of 4 [Piqueux & Christensen, 2009; Wood, 2011]. This has a significant impact on the efficiency of heat and mass transfer. Modeling of planetary interiors to predict temperature profiles, the distribution of ground ice, or assessment of subsurface habitability is dependent on identification of these parameters, which are largely unknown [Siegler et al., 2012].

Detection of water on planetary bodies could provide clues to its habitability. On Earth, extremophiles (organisms that live in conditions of extreme temperature, acidity, or alkalinity) have been observed in environments analogous to Mars [Pikuta & Hoover, 2003; Christner et al., 2000]. However, evidence of life may not be limited to bulk forms of water. Metabolic activity observed in permafrost has been linked to the presence of unfrozen films (on the order of

nanometers) that are presumably layers of adsorbed water [Rivkina et al., 2000]. Diffusion through the uppermost layer of thin films or via porous media could provide enough mobility to deliver nutrients to microbial cells and eliminate waste products [Rivkina et al., 2000; Anderson and Morgenstern, 1973; Ostroumov and Siegert, 1996].

Studies have shown that atmospheric extraction of water vapor at simulated environmental conditions analogous to Mars may not be sufficient to solely support manned missions [Schneider, 2003; Schneider & Bruckner, 2003]). Water equivalent hydrogen data, obtained from the neutron spectrometer aboard the Mars Odyssey spacecraft indicated 2-10 wt.% water in the upper meter of regolith in some equatorial regions [Feldman et al., 2004], which could provide significant amounts of consumable water.

A sample chamber is currently under development to study the behavior and stability of ground ices in the near surface of celestial bodies. The chamber will have the capability to simulate environmental conditions present in the near surface of Mars. In order to observe ice development and subsurface water diffusion at atmospheric conditions relevant to Mars, an optical sensor will be used to analyze water content. It is important for the sensor to have the capability to detect small amounts of water. This is because ice formation is expected to originate at the contact points between soil grains [Hudson et al, 2009], which are on the order of a few micrometers. Another important capability is to identify the phase of condensed water (ice, liquid, or adsorbate), which can impact diffusion and stability, particularly on bodies that exhibit large surface temperature variation. Also, unfrozen forms of water can interact dynamically with subsurface geochemistry (e.g., mineral alteration, brine formation). Therefore, the purpose of the work described in this thesis was to develop a sensor system with the ability to measure water, in order to analyze its interactions within a simulated subsurface environment.

Methods for determining water content

The tenuous atmosphere of Mars is extremely dry (global annual average water vapor content of ~10 precipitable micrometers [Smith, 2002]), dominated by CO_2 gas (95%), and has low surface pressure (~6 mbar). The effect of these conditions on ice formation and stability in the pore space between soil grains is not well understood [Siegler, 2012]. Several authors have experimentally investigated the behavior and effects of water in Mars analog soils under a variety of conditions [Janchen et al., 2006; Hudson et al, 2009; Siegler, 2012]. Some methods of directly measuring water content in soils rely on gravimetric measurements or interpretations of dielectric permittivity [Janchen et al., 2006; Zent et al., 2009].

Water content measurements by gravimetric methods are performed by measuring the wet and dry soil mass. The water content is expressed as the ratio of the weight of a sample to the dry weight. Although this method is convenient and very common, the results can be affected by mass loss due to volatiles (other than water) in the soil and temperature variability in drying ovens [Carter & Gregorich, 2006]. This method can be used to evaluate sorption capacity of porous minerals [Janchen et al., 2006], but is limited to measuring water mass and cannot distinguish where water content forms within the soil matrix.

Dielectric permittivity describes the degree to which the electrical charge distribution in a material can be affected by the application of an electric field. Water, being a polar molecule, is highly susceptible to such changes. However, the dielectric permittivity of soil is a function of the dielectric constants of air, soil minerals, water and ice; so, although changes in dielectric permittivity can be presumed to indicate changes in unfrozen water, analysis of ice content can be ambiguous because the dielectric constant of ice closely resembles dry soil [Zent et al., 2009].

While these methods are reliable, optical sensors provide a means to carry out localized measurements *in-situ*, without having to alter or displace samples, and are capable of distinguishing between liquid water, ice, and adsorbed water (thin films of water molecules on surfaces). Another important advantage of using optical sensors is the ability to evaluate the distribution of water in context with grain size. This work is not intended to replace current methods; rather, the strength of the technique presented in this thesis lies in its ability to supplement and enhance the versatility of current detection methods by providing real-time sensing of microscopic water content in dynamic, non-uniform environments.

Adsorption

Generally speaking, adsorption is a surface phenomenon that describes the adhesion of molecules to a surface due to the effects of intermolecular forces (i.e., van der Waals forces) or chemical interactions. This results in molecules (adsorbate) becoming either physically or chemically bound to a surface (adsorbent). In the case of water as the adsorbate, chemical adsorption (chemisorption) occurs first, whereby intact water molecules diffuse along a surface in a precursor state until enough energy is acquired to dissociate and form hydroxyl groups (Fig. 1.1 [a, b]). Neighboring hydroxyl groups bond (via hydrogen bonding) to incident water molecules (physisorption), forcing water in this layer into an ordered structure (Fig. 1.1 [c,d]) [Chen & Lu, 2005; Asay & Kim, 2005; Rettner et al., 1996]. Chemisorption can also occur where intact water molecules chemically bond to a surface without dissociating first. The energy associated with chemisorption is much greater than the adsorption energies of subsequent layers due to the nature of the chemical bond created between the hydroxyl groups and the surface.

Physical adsorption of water molecules to these hydroxyl groups, on the other hand, involves relatively weak intermolecular forces and is a less energetic process [Ruthven, 1984].

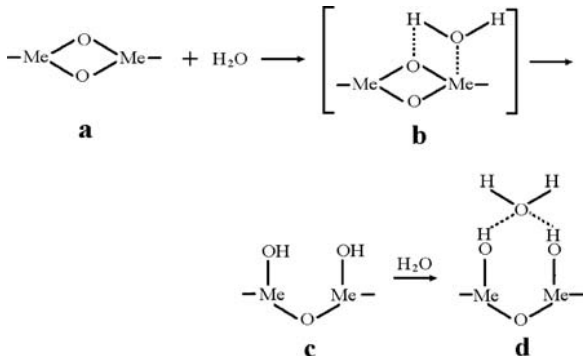

Fig 1.1. Stages of water adsorption on metal oxides—a,b) incident water molecules enter precursor state by adsorbing to a surface; b-c) adsorbed molecules disassociate to form hydroxyl groups; c-d) water molecules form hydrogen bonds with neighboring hydroxyl groups [Chen and Lu, 2005]. A similar process occurs on silica surfaces [Bogdan, 2000]

Adsorption of water vapor is a common occurrence on Earth and pervades at various combinations of temperature and humidity—even the driest environments on Earth will exhibit some adsorbed water on surfaces. Therefore, it is assumed that other planetary bodies (with rocky surfaces) would exhibit similar processes. For example, significant amounts of hydrogen at the equatorial regions of Mars could be due to water adsorption on mineral grains [Mohlmann, 2003; Jakosky et al., 2005].

The main objective of this work was to determine if implementation of optical sensors would provide enough sensitivity to detect and quantify small volumes of bulk water or films of adsorbed water.

Thesis Organization

To understand the process by which light confined to the interior of a fiber optic cable interacts with an external medium, Chapter 2 describes the fundamentals of internal reflectance spectroscopy and optical sensors. Chapter 3 presents an overview of the experimental facility and details how each measurement was performed. Finally, Chapter 4 presents the results of the experiments and a discussion of their implications.

Ch. 2 Techniques and Materials

Vibrational Absorption of Water in the Near Infrared

The absorption spectrum of water from the ultra-violet to the far infrared is highly complex. Being a non-linear molecule, water has three vibrational degrees of freedom (i.e., 3*N*-6 vibrations, where N [the number of atoms]=3), which correspond to the three fundamental molecular vibrations (symmetric stretch [ν_1], antisymmetric stretch [ν_3], and bending [ν_2]). Each of these vibrational modes has an associated frequency and interacts with light in the mid-infrared region (MIR) of the electromagnetic spectrum at unique wavelengths, i.e., 3.1, 2.9, and 6.1 μm, respectively. Combinations and overtones of these vibrations occur in the near-infrared region (e.g. 1.45 μm [$\nu_1+\nu_3$] and 1.94 μm [$\nu_2+\nu_3$]) (Fig 2.1). When water interacts with electromagnetic radiation at these frequencies, absorption will occur. The various phases of water have similar absorptions in the near-infrared (NIR) but exhibit either phase-dependent shifting or variations in absorptivity at a particular wavelength. These differences are presumed to be due to the configuration in which molecules can vibrate as a function of phase. For example, the nature of the crystalline structure of ice (when compared with liquid water) results in absorptions that are shifted to longer wavelengths. In general, the absorption of light by a medium is expressed by the Beer-Lambert relation:

$$\frac{I}{I_0} = e^{-\alpha x} \tag{2.1}$$

where I/I_0=spectral transmission and x=path length

I_0 represents the intensity of light prior to entering a region, of length x, where absorptions will occur. The absorption coefficient, α, describes the strength of absorption and is the product of

molar absorptivity and molar concentration. The absorption coefficient of liquid water has been determined to be $\alpha \sim 114$ cm^{-1} at $\lambda = 1.94$ μm and $\alpha \sim 26$ cm^{-1} at $\lambda = 1.45$ μm [Curcio & Petty, 1951]. These values were used for all calculations in this work.

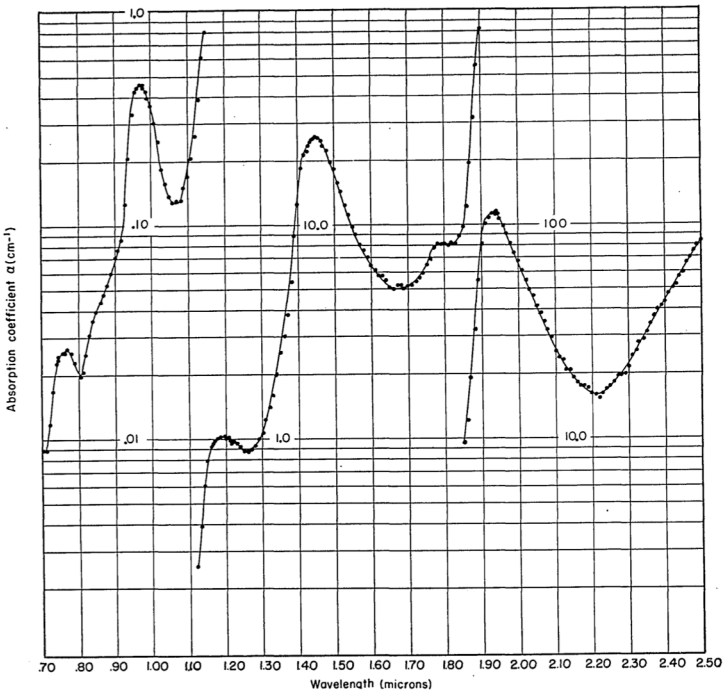

Fig 2.1. Water absorption in the near-infrared of liquid water at 20°C. Spectra are plotted as absorption coefficients with respect to wavelength (in micrometers). [Curcio & Petty, 1951].

Internal Reflection Spectroscopy

Internal Reflection Spectroscopy refers to a sampling technique that utilizes the evanescent field (also referred to as the evanescent wave), created at an interface where total internal reflection occurs, to analyze light interactions with matter. Total internal reflection occurs when light propagating within a medium of higher refractive index interacts with a medium of lower refractive index at angles greater than the critical angle, θ_{crit} (Fig 2.2). The critical angle is defined as the angle of incidence for which the angle of refraction is 90° (Eq.

2.3), a derivative of Snell's law, and is determined by the refractive indices of the media involved. Although light is *totally* reflected at the interface between two media, a portion of the

$$\theta_{crit} = \sin^{-1}\left(\frac{n_2}{n_1}\right) \tag{2.3}$$

where n_1=originating medium
n_2=refracting medium

electromagnetic field, known as the evanescent field, penetrates from the originating medium to the other. This field decays exponentially with distance from the interface of the two media. The distance the field extends into the second medium is referred to as the penetration depth, d_p, and is a function of vacuum wavelength [λ], the ratio of refractive indices [$n_{21}=n_2/n_1$], and incidence angle [θ] (Eq. 2.4). The penetration depth is defined as the distance required for the

$$d_p = \frac{\lambda}{2\pi n_1 \sqrt{\sin^2(\theta) - n_{21}^2}} \tag{2.4}$$

amplitude of the electric field to fall to 1/*e* of its value at the surface. The amplitude of the electric field, E, is described in terms of d_p, E_0, and z (Fig 2.3), where E_0 is the amplitude of the electric field at z=0 [Harrick, 1967]. The penetration depth is an important parameter for this work because it provides context for all spectral measurements. Furthermore, the water absorption bands in the near-infrared, i.e., λ =1.94 and 1.45 μm, are quite broad so penetration depths can vary by as much as 15% for a given angle within ±.1 μm of each wavelength. However, the penetration depth, over the range of angles used in this study, varies by an order of magnitude (Fig 2.4). Due to the design of the experimental facility, incidence angles could only be constrained to the range of angles that propagate through the optical cable. This caused

quantitative analysis of the depth of the medium to be somewhat limited due to the variability in penetration depth.

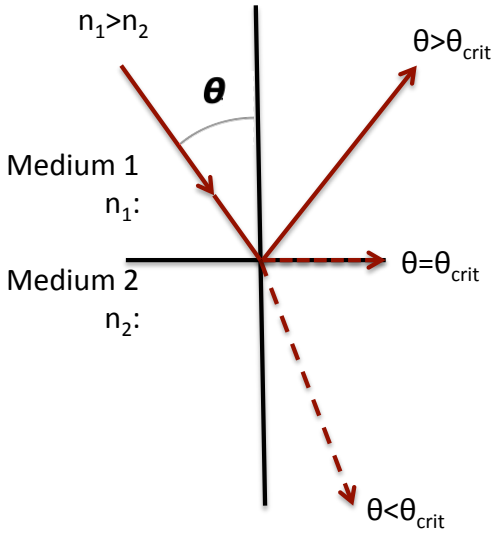

Fig 2.2. Conditions when light entering a medium of lower refractive index will undergo total internal reflection. The dashed line represents light that refracts at the interface.

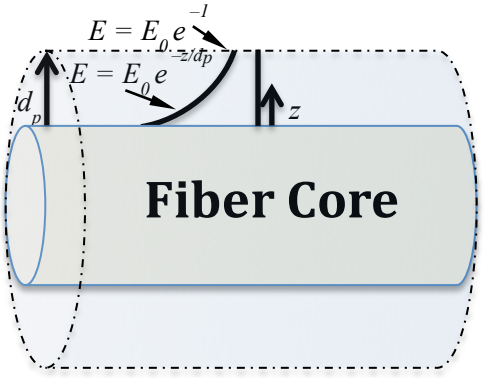

Fig 2.3: Evanescent field at core boundary

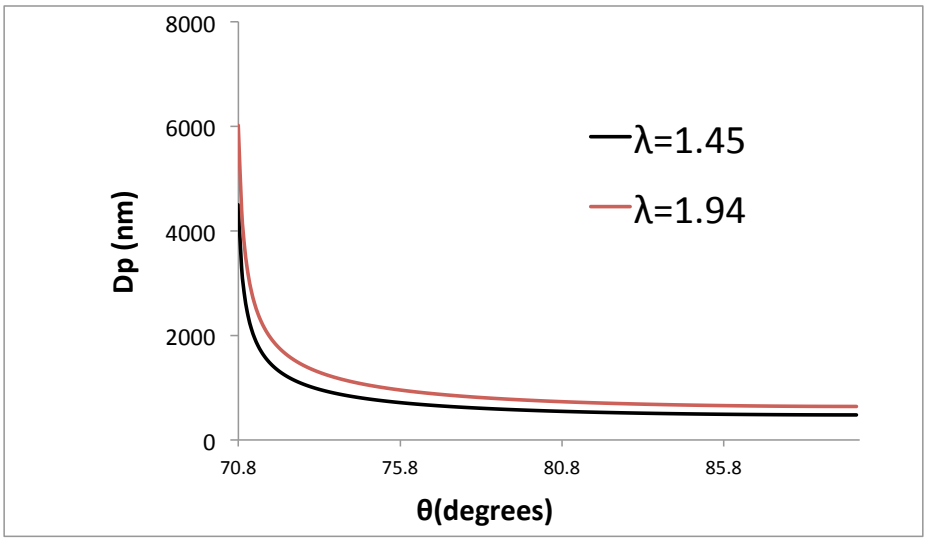

Figure 2.4: Penetration depth as a function of θ at λ =1.94 µm and 1.45 µm

Optical Cable Properties

Most optical cables have several layers (Fig 2.5) surrounding the core that provide both optical and mechanical advantages. The first layer or cladding is a material with a lower refractive index than the core (allowing for total internal reflection) and is generally either a polymer or glass. The next layer (primary coating) commonly referred to as a buffer, provides protection and elasticity. Lastly, a secondary coating or jacket forms the thickest layer to protect the core from excessive bending and breaking. Low-OH fibers were used in this study and were obtained from Thorlabs, Inc. (Newton, NJ). The cable properties and transmission spectrum are listed in Table 2.1 and displayed in Fig. A.1 respectively. The index of refraction of the core and cladding used in this study were based on specifications obtained from the manufacturer.

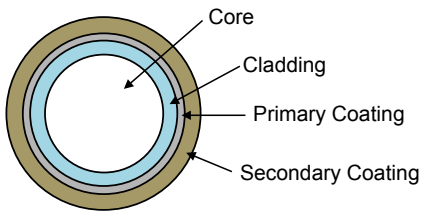

Fig 2.5: Cross-section of a fiber optic cable

Fiber optic sensors

Spectroscopic measurement with fiber optic sensors is a convenient means to conduct analysis in real-time and *in-situ*. These sensors have a wide variety of applications ranging from groundwater and organics detection to monitoring alcohol content and air pollution [Harrington, 2004; Degrandpre & Burgess, 1990; Inaba et al., 1979; Simhony et al, 1986; Xiong & Sisler, 2009]. There are several types of fibers available for much of the electromagnetic spectrum; therefore, selection of an appropriate fiber depends on the transmission properties of the optical

Table 2.1: NIR Optical Cable Properties

Spectral Range	.4 – 2.2 μm
Core Diameter	1000 μm
Length	2 m
Core Material	Pure silica (SiO_2)
Core Refractive Index	1.457
Cladding Material	Hard-polymer
Cladding Thickness	17 μm
Cladding Refractive Index	1.375
Numerical Aperture	.48 ± .02
Manufacturer	Thorlabs, Inc. (BFL48)

glass and the spectral region of interest [Saito and Kikuchi, 1997]. In general, there are two types of fiber optic sensors—extrinsic and intrinsic. Extrinsic sensors primarily utilize the optical cable to transmit light. In other words, the *sensing* component does not directly involve the optical cable (Fig 2.6a). Alternatively, with an intrinsic sensor system, the optical properties

of the cable have been altered such that the core is actively involved in the detection of components within a medium via the evanescent field (Fig 2.6b). An advantage of using an intrinsic system is that light interaction within the medium is limited by the depth of the evanescent field generated at the surface of the fiber core. This is particularly beneficial when analyzing highly absorbing media. For this work, intrinsic sensors were chosen primarily to spatially constrain observations of small volumes of water. These inherent features of intrinsic sensors provide unique capabilities that will be significant for future analysis of soil systems (e.g., ice accumulation at soil grain contact points).

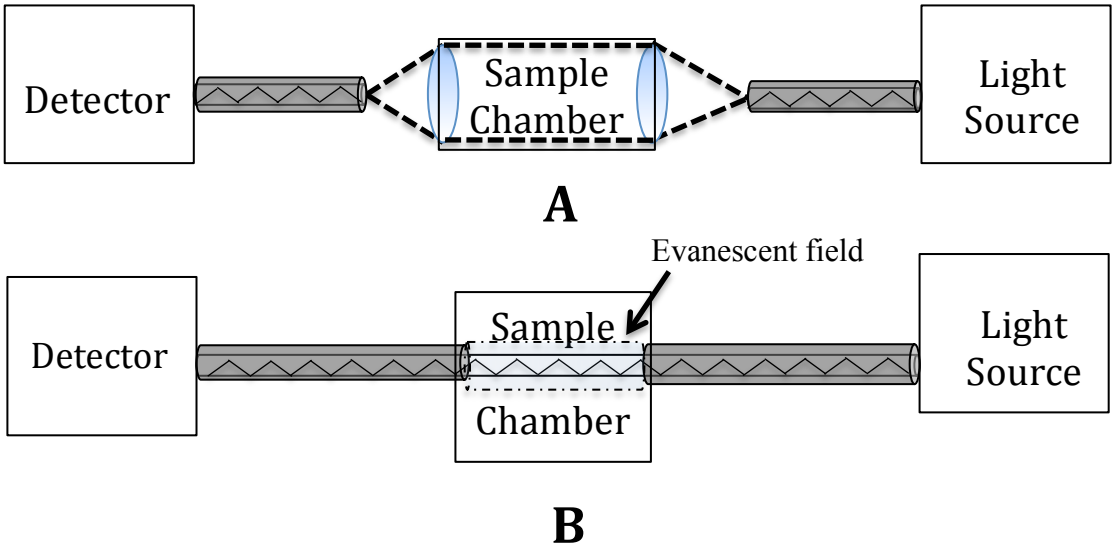

Fig 2.6: Optical fiber sensor systems. A) Extrinsic and B) Intrinsic sensor

Ch. 3 Experiment design and description

Experimental Facility

The experimental facility (Fig. 3.1) used in this work included a Vector 33 Fourier Transform Infrared (FTIR) Spectrometer, a Harrick Scientific Fibermate 2 fiber optic coupler, a NIR optical cable, and a sample chamber. The spectrometer is equipped with a deuterated L-alanine doped triglycine sulfate (DLaTGS) pyroelectric detector, a common component used in the near-infrared region (1.2-2.5 μm). The NIR cable was connected to the spectrometer via the fiber optic coupler, using SMA (SubMiniature version A) connectors. Modification of the optical cables was required to enable sensing. This involved altering a small section of the optical cable to expose the fiber core or internal reflectance element (IRE). This process is explained in detail in the following sections. The IRE was housed in the sample chamber where all measurements were obtained.

Optical Path

An important consideration of this design was to understand the effects of the optical path of light on detection. Figure 3.2a displays the optical path of a standard FTIR (Fourier-Transform Infrared) spectrometer without the addition of a fiber-optic coupler. Using a coupler (Fig 3.2b) redirects light such that, rather than pass directly through the sample compartment to the detector, light enters the coupler, reflects off a series of mirrors and exits via an SMA termination (Fig 3.2b). Once an optical cable is attached to the coupler via mating SMA terminations (Fig 3.1), light enters and propagates within the cable and re-enters the coupler at another SMA termination. Once again, light is reflected via a series of mirrors, exits the coupler,

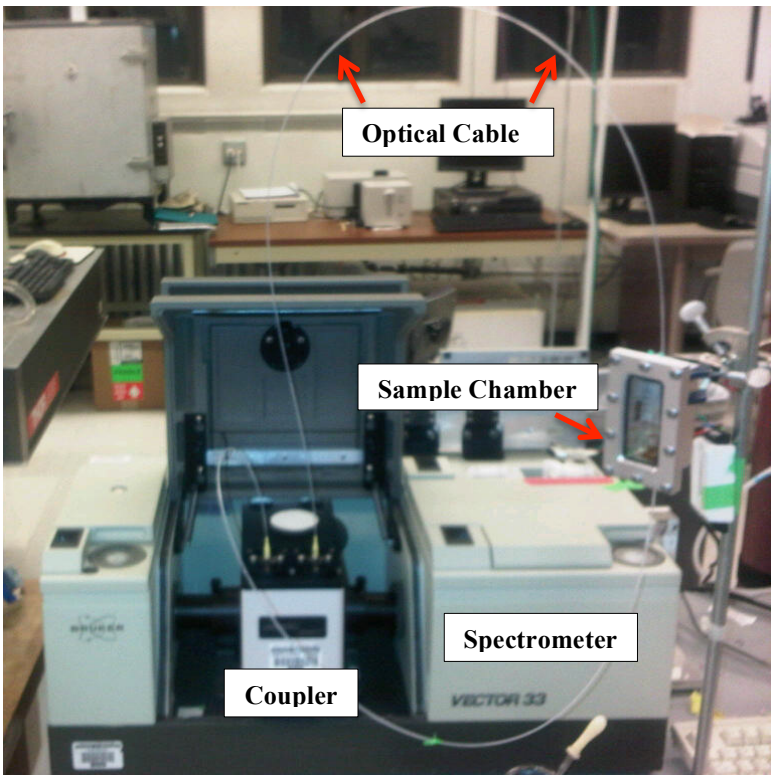

Fig 3.1: Facility setup including sample chamber and NIR optical cable. This configuration was used for liquid water and vapor measurements.

and is guided to the detector. Transmission losses are inherent in optical systems and vary as a function of cable length and optical path. Therefore, a major issue throughout this project was ensuring enough light was transmitting through the system to register at the detector. To ensure optimal detection, cable lengths were minimized to two meters. This resulted in transmission values of 4.0 and 2.5% at λ =1.94 and λ =1.45 μm, respectively, of the maximum transmission capability of the spectrometer. These values were acquired at dry conditions (relative humidity ~0.1±3%) when the fiber core (IRE) was exposed.

Sample Chamber

The sample chamber was designed to withstand a variety of temperature and humidity conditions, provide adequate structure for cable integration, and adapt to multiple configurations.

Several factors determined the size of the sample chamber. In order to ensure humidity readings were representative of the humidity conditions present at the surface of the IRE (Fig 3.3), the internal volume of the chamber was minimized to 52 cm^3. This dimension was chosen to provide adequate space for installation/removal of a humidity sensor, placement of two optical cables (NIR and MIR [see Ch. 5]), and sufficient volume to submerge the sensors in a variety of media (e.g. glass beads, Mars analog soils) for future experiments. Data from preliminary work with other chamber designs (~440 cm^3), showed inconsistencies in spectra at assigned humidity levels. This suggested that the time required for water vapor to equilibrate within the volume of the chamber was greater than expected. Therefore, the volume of the sample chamber was reduced to 52 cm^3, which decreased the equilibration period to ~30 minutes. The lid of the chamber was made of clear glass and allowed the interior of the chamber to be viewed. This feature was useful because a) it provided a direct way to continually inspect the IRE for damage, b) allowed viewing of the water level for liquid water measurements, and c) afforded visual assessment of condensed water during relative humidity measurements. Integration of the sample chamber with the experimental facility occurred in two phases. The first phase involved construction and cable installation; the latter phase involved acquiring spectral measurements which were taken under separate facility configurations—one at room temperature conditions, the other at freezing conditions.

Phase One

This phase contained the construction and component integration of the sample chamber. Because the hard-polymer cladding of the optical cable could only be removed by melting and the chamber needed to achieve freezing temperatures, aluminum was chosen for

A

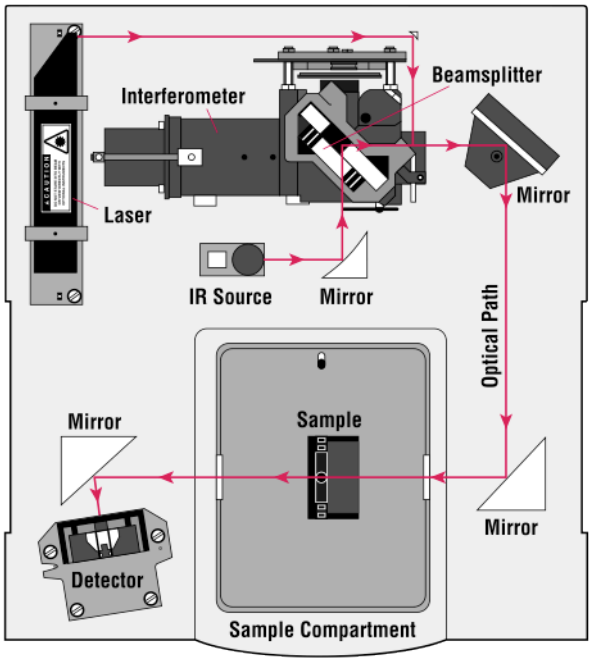

B

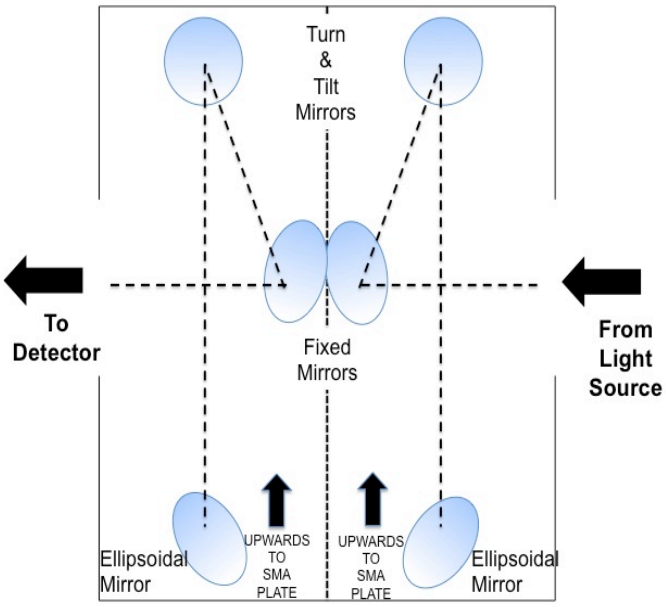

Fig 3.2: Top-down view of optical path in facility. A) Path within FTIR spectrometer [Courtesy of Thermo Nicolet Corporation]. B) Path within optical coupler. The optical coupler resides inside the sample compartment shown in A).

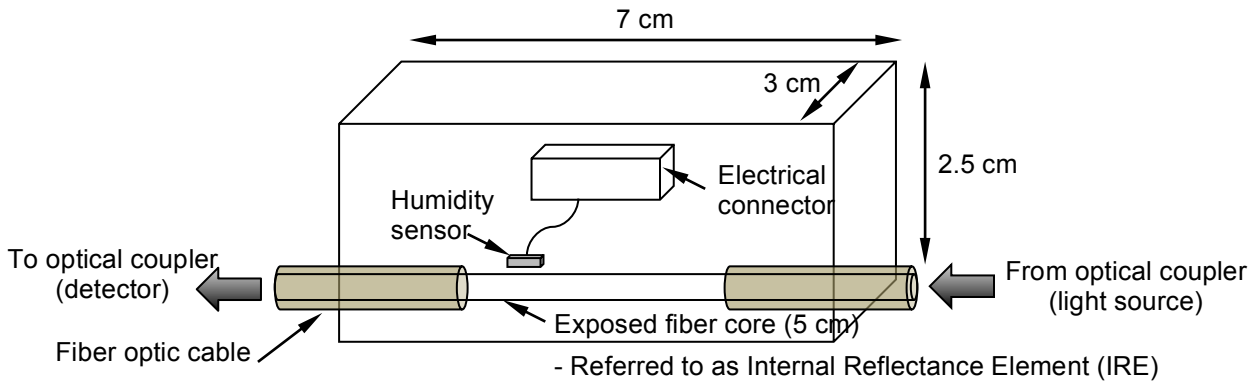

Fig 3.3 Sample Chamber Dimensions and Components

construction because it is thermally conductive as a heat sink and was easily machined. Three of the sidewalls were drilled to accommodate SMA connectors at the ends of the optical cable, ports for gas-input and venting, electrical connections for the humidity sensor, and access ports for a fiberscope (not pictured in Fig 3.3). After drilling, the optical cable was epoxied to mounting posts (~3 mm above the chamber floor), which were in turn epoxied to the floor of the chamber. The dimensions of the chamber also provided enough thickness to the chamber walls (~3 mm) such that portions of the cable could be epoxied inside the cable ports. Epoxying the cables in this manner served two purposes. The first was to provide an added layer of protection to the IRE at the cable ports. Silica glass fibers are extremely delicate and can fracture if torqued or subjected to excessive vibrations. Furthermore, epoxying the clad portions of the cable *within* the interior chamber was a means to dampen any strain in close proximity to the IRE. The other reason was to ensure a hermetic seal at the cable ports. A D-subminiature nine (DB9) electrical feed-through was also epoxied to the wall of the chamber (Fig 3.4). Two attachments were used at each end. The internal mate was soldered to the humidity sensor and the external mate was soldered to the data acquisition device (DAQ). Each of the attachments plugged directly into the

chamber-wall feed-through. This component was designed so that the humidity sensor could be removed for other configurations.

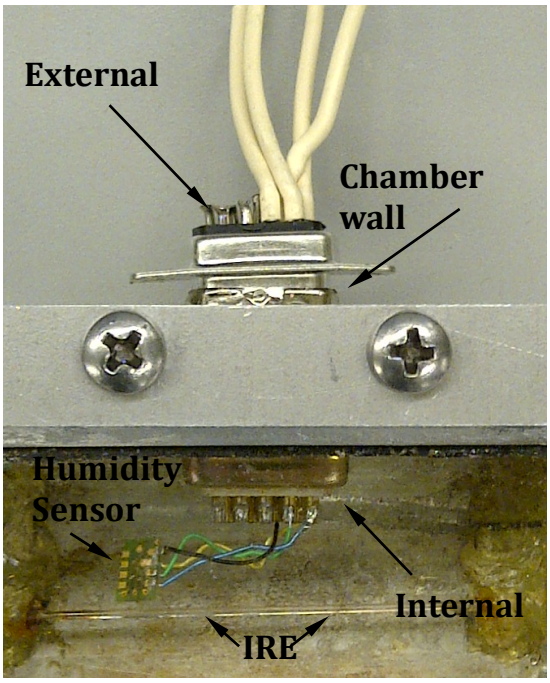

Fig 3.4 Electrical Connections

A small hand-held butane flame torch was directed at a 5cm section of the optical cable (located between the mounting posts) to remove the external layer. This allowed the buffer and cladding layers to melt away, exposing the core. This process took several seconds after which the IRE was rinsed with alcohol and dried. After cladding removal, the removable lid (with viewing window) was attached to the chamber at all times to protect the IRE from dust/dirt and mechanical damage. A rubber seal was placed between the body of the chamber and the lid to maintain a hermetic seal. The lid was anchored to the body of the chamber by several screws.

Two Teflon-coated ports provided access for a fiberscope instrument. This allowed the interior of the sample chamber to be viewed at high magnification when the lid was attached. When not in use these ports were sealed with silicone plugs.

Phase Two

Spectroscopic measurements of liquid and adsorbed water were obtained using the same orientation (Fig 3.5) at room temperature (~22°C). For humidity measurements, a Sensirion capacitive-type humidity sensor was placed 3 mm from the IRE (Fig. 3.3) to measure relative humidity (RH). For liquid water measurements, the sample chamber was first purged with dry nitrogen to provide a reference spectrum at dry conditions (relative humidity ~0.1±3%). Next, the chamber was filled with water in 5 mm increments. This process was repeated until the IRE was completely immersed in water. A transmission spectrum was taken at each increment and normalized to the reference spectrum. An additional method used when taking liquid water measurements involved flowing dry nitrogen over portions of the sensor that were not yet immersed in water. The objective of this approach was to reduce water vapor adsorption on the exposed portions of the sensor. Again, spectra were taken at 5 mm increments until the sensor was completely immersed in liquid water.

Similarly, water vapor adsorption measurements were initialized by purging the sample chamber with dry nitrogen prior to acquiring a reference spectrum. Subsequent transmission spectra were taken at relative humidity values ranging from 8.1-96%. The humidity was controlled using two methods. It was difficult to maintain stable humidity conditions for more than a few minutes at very dry conditions (RH<20%), so separate techniques were required to

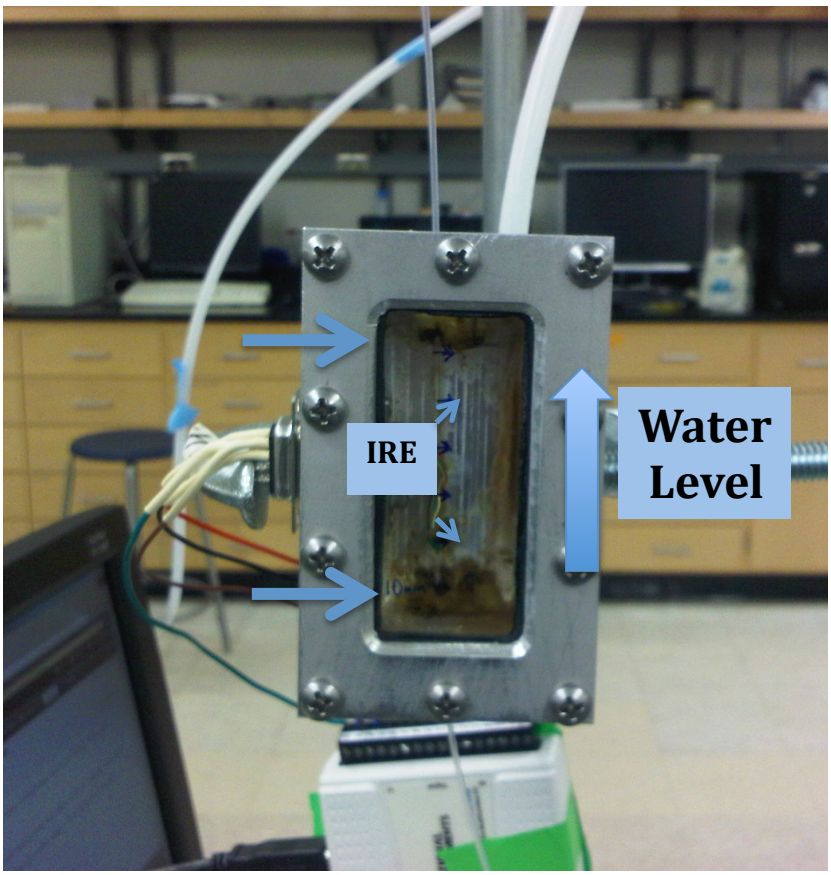

Fig. 3.5 Sample chamber configuration for liquid water measurements

obtain spectra at dry conditions and humid conditions. Low humidity measurements were obtained by adding small amounts of liquid water via the gas-inlet port then re-sealing the chamber. This process facilitated increasing the humidity at small increments and conserved time and resources (e.g., nitrogen gas). This procedure was not necessary at higher humidity regimens so instead a "bubbler" system was used to vary humidity. This system involved passing nitrogen gas through water such that the exit gas contained a mixture of water and nitrogen. This was accomplished by flowing dry nitrogen gas into a flask filled with liquid water. The entering gas line was positioned at the base of the flask, whereas, the exiting line was positioned at the top of the flask. Both lines were secured to the flask with a rubber stopper. The

concentration of water in the mixture is controlled by gas pressure—as bubbles of nitrogen ascend and mix at low pressure (<2 psig), the resulting gas becomes enriched with water vapor. This mixture was connected via plastic tubing to the sample chamber for several seconds, after which the chamber was re-sealed. Once humidity conditions stabilized inside the chamber (fluctuations decreased to ±0.5%) a transmission spectrum was acquired. This process was repeated at ~10% humidity intervals.

A separate configuration was used to measure spectral absorptions by water in the ice phase. Thermoelectric coolers (TECs) were used to cool the chamber to freezing temperatures. This was accomplished by bonding the TECs to an aluminum block (used as a primary heat sink) with a high-density polysynthetic thermal compound. The sample chamber was oriented horizontally and placed on the TECs. The aluminum block was then placed in an ice bath (Fig 3.6). An ice bath served as a secondary heat sink in order to ensure that the ceramic tiles of the TECs would provide sufficient cooling to the sample chamber. With this system in place, temperatures inside the sample chamber were able to stabilize around -5°C.

Ice measurements were initialized in the same manner as previous measurements to acquire reference spectra. After which, the lid was removed and the sample chamber was filled with liquid water. The chamber was then cooled to temperatures at/below 0°C. Once water within the chamber was completely frozen, a spectral measurement was taken. Next, the sample chamber was heated to return the ice to the liquid phase and further spectral measurements were acquired. The process of cooling the chamber was repeated and measurements were taken again in the ice phase. It was important to assess temperature dependency (if any) on spectral absorption within each phase. Absorptions in the solid phase at longer wavelengths (λ =15-20 μm) from -15° to -5°C depend strongly on temperature [Warren & Brandt, 2008]. It was

desirable to determine if temperature dependency within phase or intermediate spectral signatures indicating the transition from the liquid phase to the solid phase could be observed. Measurements indicate that temperature variations within each phase did not affect absorption in the -5° to 32°C temperature range.

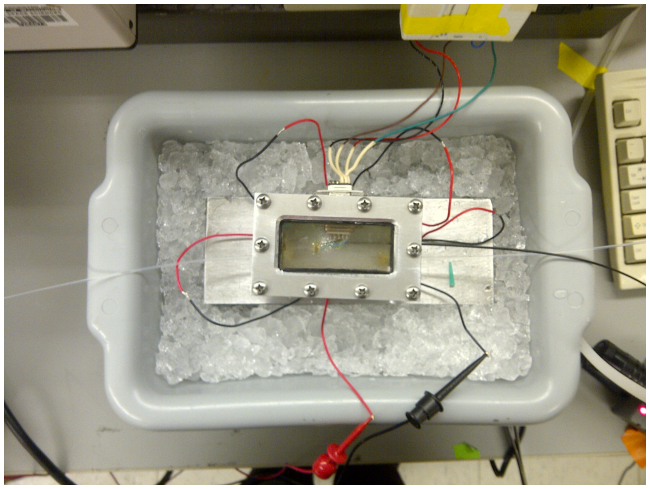

Fig 3.6: Facility setup including sample chamber and NIR optical cable. This configuration was used for ice measurements.

Thermoelectric coolers were chosen for temperature variation. These coolers were effective at providing timely temperature changes within the sample chamber. By using thermoelectric coolers, freezing/thawing liquid water only took a matter of minutes and facilitated collecting measurements in an efficient manner.

Electrical Components

The humidity sensor was controlled via a DAQ (acquired from National Instruments, Inc.) by a graphical user interface (GUI) designed in Lab view (Fig 3.7). The sensor transmitted relative humidity and temperature data at a frequency of 10 Hz. The GUI was used to monitor the temperature and relative humidity during water vapor adsorption measurements. An external

thermometer was used for temperature measurements when use of the temperature/humidity sensor was not practical (i.e., during liquid water and ice measurements).

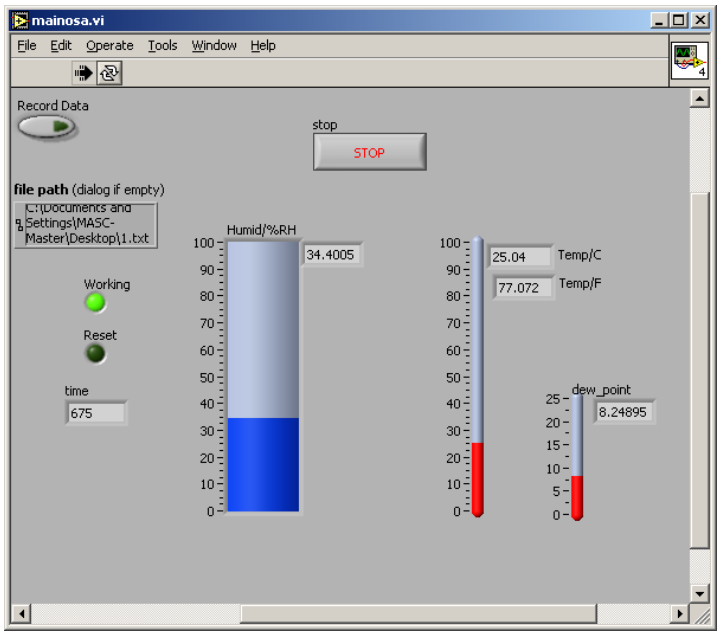

Fig 3.7 Graphical User Interface for Temperature/Humidity Sensor

Ch. 4 Results and Discussion

Evanescent Wave Absorption Coefficient

Absorption due to the evanescent wave is proportional to the free-space absorption coefficient, α, (Eq. 4.1) where γ(ϕ) represents the evanescent wave absorption coefficient [Zhang et al., 2009]. This relationship describes absorption at the core interface at wavelength, λ, launched at angles, ϕ. The parameters *r*, n_1, and θ_{crit} are the core radius, core refractive index, and critical angle, respectively [ϕ=π/2-θ]. Incidence angles are defined as the angle between incidence light rays and the optical axis of the fiber core (for further clarification see Fig. A.2).

$$\gamma(\phi) = \mathcal{R}\alpha \tag{4.1}$$

where

$$\mathcal{R} = \frac{\lambda}{2\pi r n_1}\left(\frac{\phi^2}{(\frac{\pi}{2}-\theta_{crit})^2\sqrt{(\frac{\pi}{2}-\theta_{crit})^2-\phi^2}}\right) \tag{4.2}$$

Absorption of water via the evanescent wave is a function of IRE length (or path length), and is similar to free-space absorption in terms of the Beer-Lambert relation shown in Eq. 2.1. For evanescent wave absorption, the term α is replaced by γ (Eq. 4.3) to describe transmission with respect to the evanescent field. As with Eq. 2.1, the term *x* represents the path length or IRE length. Therefore, Equation 4.3 can be used to predict transmission.

$$\frac{I}{I_0} = e^{-\gamma x} \tag{4.3}$$

Figure 4.1 illustrates that the difference between evanescent wave and free-space absorption resides in how the path length is defined. As mentioned in Chapter 2, free-space

absorption is a function of the length of the sample cell. Similarly, evanescent wave absorption is a function of the length of the IRE. Additionally, the $\mathcal{R}$ term of the evanescent wave absorption coefficient assumes water is in a bulk form and the penetration depth is much smaller than the distance the medium extends from the surface of the IRE. In other words, the evanescent wave absorption coefficient, as defined in Equations 4.1 and 4.2, would not apply to adsorbed water layers (penetration depth >> distance medium extends from IRE surface) and could not be used to predict transmission as a function of relative humidity in the near-infrared. Also, the evanescent wave absorption coefficient assumes the distribution of the medium is homogenous. Equation 4.1 could be used to predict transmission in ice; however, evanescent wave absorption coefficients were only calculated for liquid water measurements.

Using Eq. 4.1 and 4.2, the theoretical value of the evanescent wave absorption coefficient at λ=1.94 μm was determined to be .044 cm^{-1}(r=500 μm, n_1=1.4, n_{2water}=1.3, $\phi_{W.AVG}$=.171 rad, 90-θ_{crit}=.337) and .007 cm^{-1} at λ=1.45μm. This can be compared with values of .038 cm^{-1} and .009 cm^{-1}, respectively, that were calculated (using Eq. 4.3) from transmission measurements in Fig 4.2, where x=5cm. Because the distribution of incidence angles was poorly constrained, an average value was calculated. This value, $\phi_{W.AVG}$, was weighted by the penetration depth for the range of angles used (Fig 2.4). Figure 4.2 contains spectra of liquid water absorbance (log [1/T]), within the evanescent field of the IRE. The length of the IRE was 5 cm. Each curve, normalized to the transmission curve obtained at RH=0.1±3%, displays absorbance at 10% increments of surface coverage until the IRE is completely immersed. As can be seen in Fig 4.2, absorbance increases with IRE coverage.

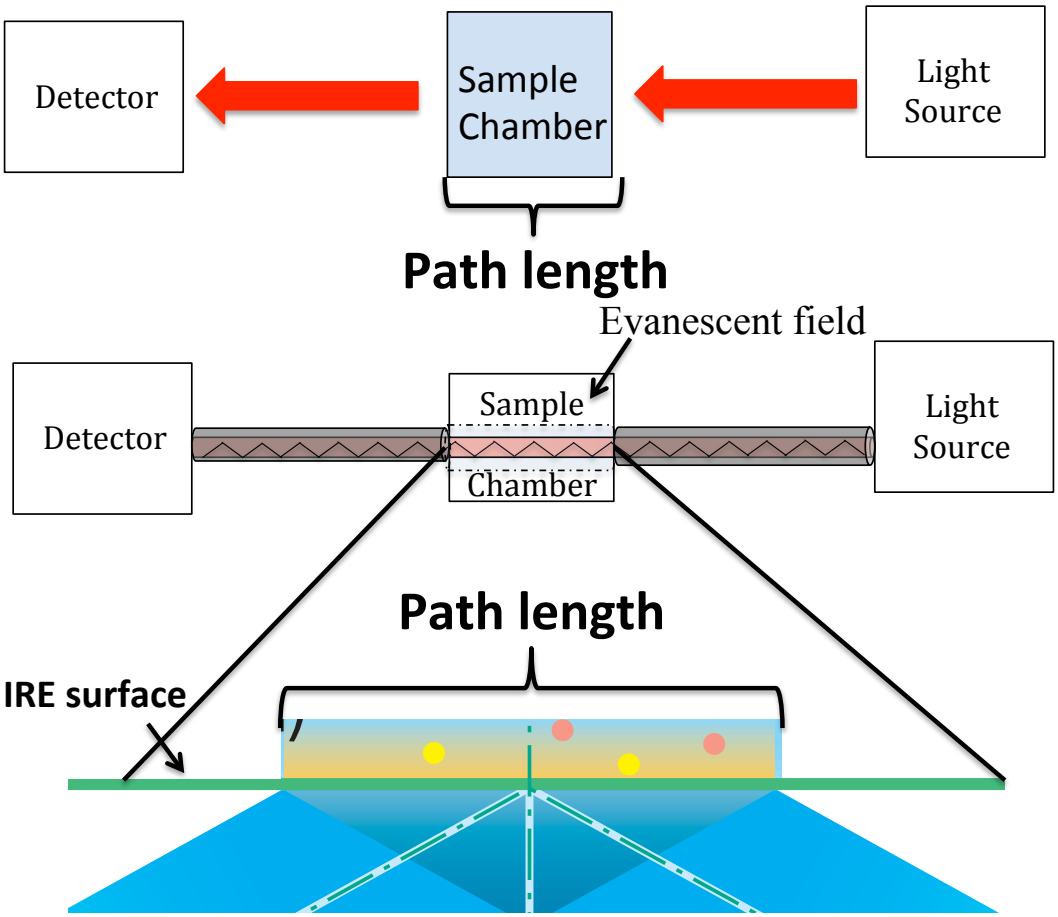

Fig 4.1: Free-space absorption vs. Evanescent wave absorption

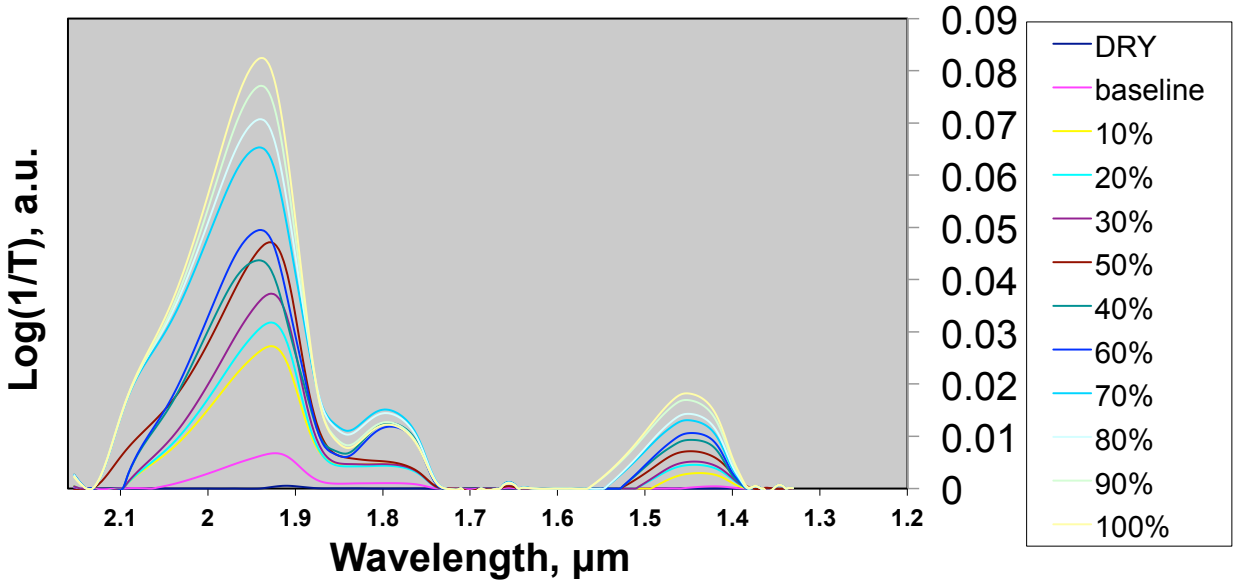

Fig 4.2: Near infrared spectra of liquid water showing absorbance as a function of surface area coverage of IRE (increasing upwards), IRE length = 5cm. "Dry" refers to the driest possible condition in the sample chamber (i.e., RH=0.1±3%), whereas, "Baseline" refers to the condition when liquid water was present in the sample chamber but not in contact with the IRE.

Eq. 4.3 can be used to predict the absorbance (log [1/T]) as a function of IRE coverage. Although the length of the IRE did not change, sections of the IRE that were immersed in water varied in 10% increments. Figs 4.3 and 4.4 show peak absorbance plotted with respect to IRE coverage in liquid water. The yellow line displays theoretical values of absorbance (based on evanescent wave absorption coefficient calculations) and measurements are displayed in blue. This shows that γ is a useful parameter in estimating evanescent wave absorption with respect to IRE length and incidence angle.

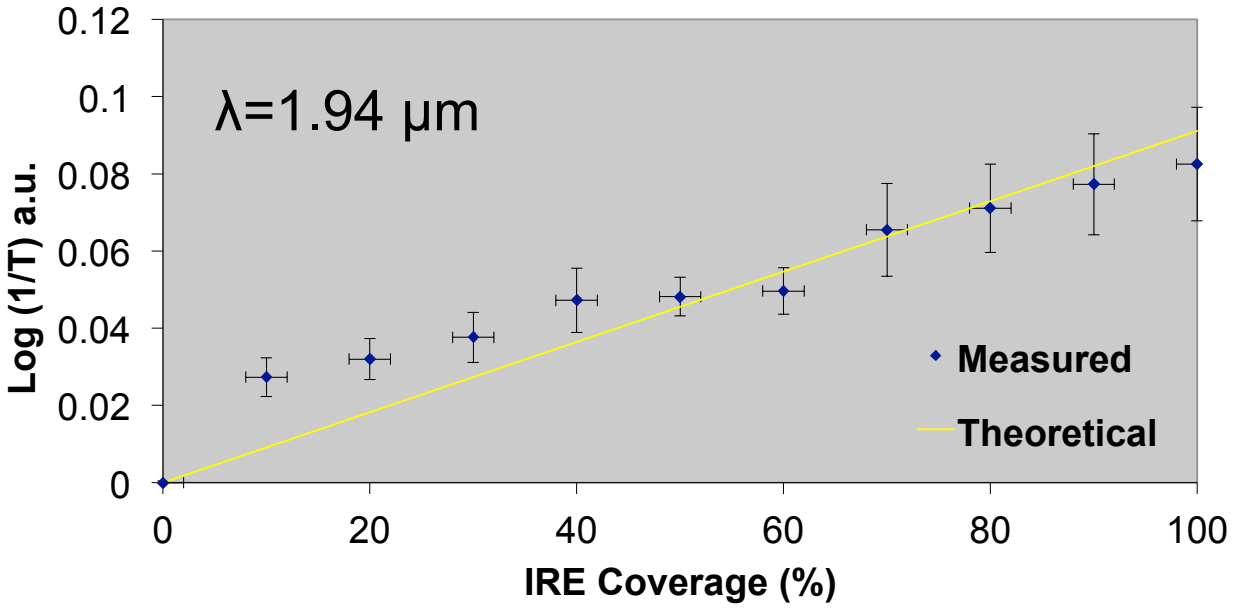

Fig 4.3 Absorbance of liquid water (λ=1.94μm, IRE length = 5cm)

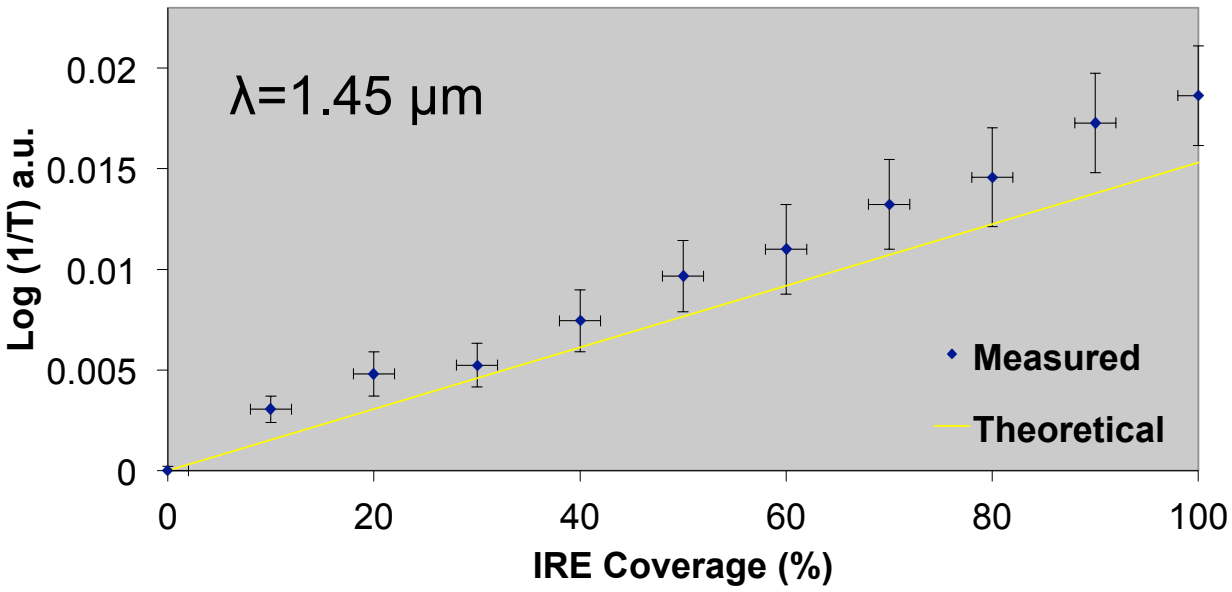

Fig 4.4 Absorbance of liquid water (λ=1.45μm, IRE length = 5cm)

Adsorbed Water Measurements

Figures 4.2-4.4 demonstrate that optical sensors are sensitive to water in the liquid phase, however, in certain environments, water adsorbed to surfaces is more pervasive than its liquid form. Layers of adsorbed water can be used as a proxy for humidity conditions in that an increase in the number of layers can be associated with an increase in relative humidity [Asay and Kim, 2005]. Therefore, spectral measurements were taken at a range of humidity conditions to determine if adsorbed water could be observed and quantified using an intrinsic optical sensor. Figure 4.5 shows absorption due to water adsorbed on the IRE as a function of relative humidity (P/P_{sat}), which is defined as the ratio of vapor pressure to saturation vapor pressure for a given temperature. Spectral absorptions in Figure 4.5 closely resemble those of liquid water, indicating the presence of water adsorbing to the surface of the IRE in the absence of bulk water. Increasing relative humidity correlates to an increasing concentration of water molecules on the surface of the IRE as adsorption layers (adlayers) build. At high humidity levels, there can be as many as ten adlayers present on the surface of the IRE, each layer having the depth of a single water molecule (~2.82 angstroms, the mean van der Waals diameter of water) [Asay and Kim, 2005].

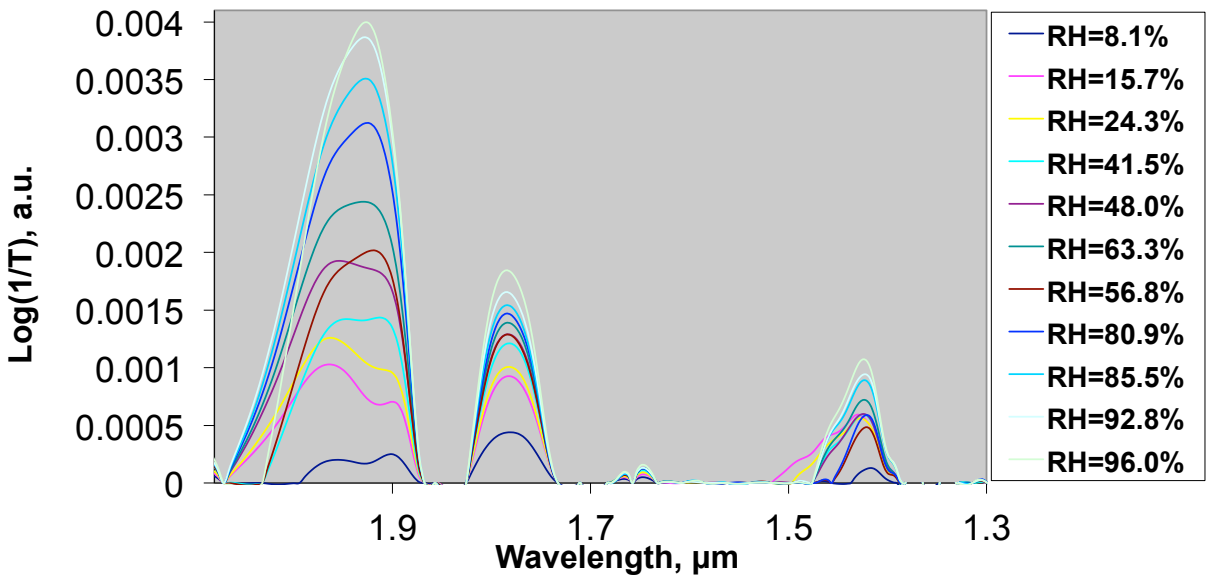

Fig 4.5: Near-infrared spectra of absorbed water showing increased absorption as a function of relative humidity (IRE length = 5cm)

To determine the contribution of adsorbed water on spectral absorption in the presence of liquid water, dry nitrogen was flowed over portions of the IRE that were not immersed in bulk water (Fig 4.6). Reduced absorbance indicates that less adsorbed water (not necessarily a lack of adsorbed water) was present on the IRE than when flowing nitrogen was not used. The first layer of adsorbed water chemisorbs to the surface of silica surfaces [Bogdan, 2000], so nitrogen alone would not remove all adsorbed water. However, the amount of adsorbed water displaced from the IRE with flowing nitrogen is significant. The difference in magnitude of the absorbance curves in Figure 4.6 is similar to the max absorbance of adsorbed water (Fig. 4.7).

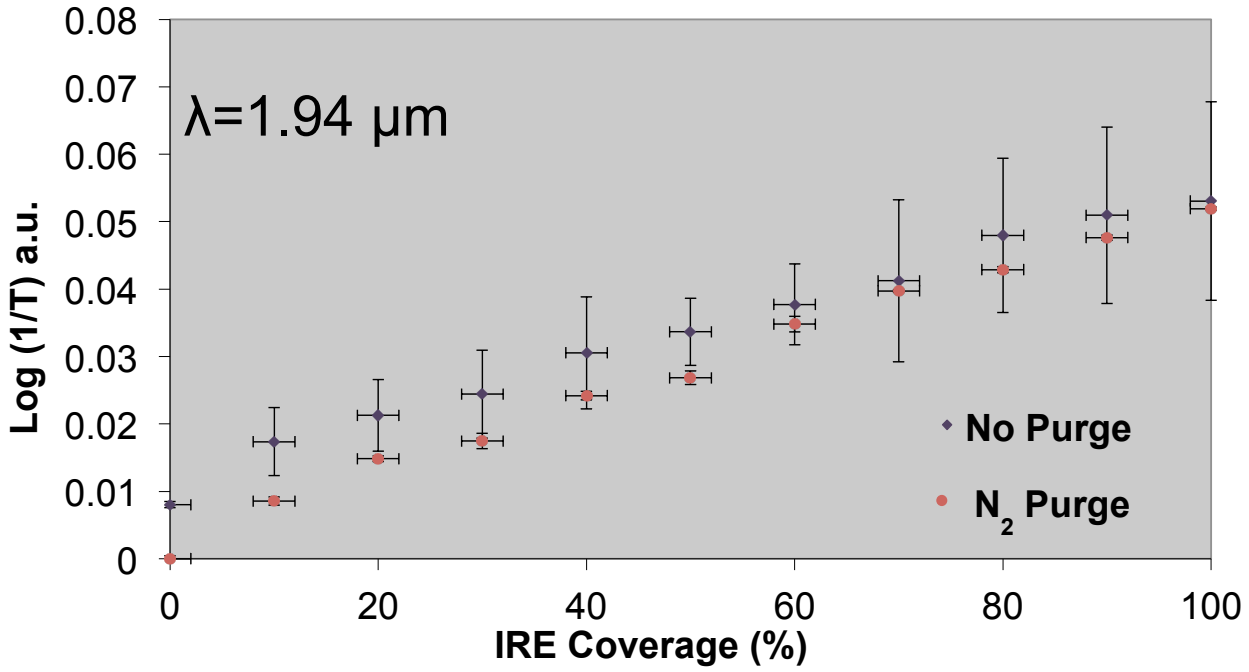

Fig 4.6: Near-infrared spectra of liquid water showing peak absorbance decrease with drying of exposed IRE sections at λ=1.94μm (IRE length = 5cm). The top curve displays spectral absorption as a function of IRE coverage under standard conditions (no flowing nitrogen) and the bottom curve shows spectral absorptions with flowing nitrogen.

Figure 4.7 shows peak absorbance at λ=1.94 μm of adsorbed water plotted with respect to relative humidity (P/P_{sat}) and absorbance at λ=1.94 μm of liquid water with respect to IRE coverage. At saturated conditions, when liquid water was present in the sample chamber but not in contact with the IRE, liquid water results (absorbance=.007 a.u. at "0%" coverage) agree well with absorbance measurements at the highest measured relative humidity (absorbance=.004 a.u at RH=96%.). The plotted results show an increase in absorbance by a factor of 10 (when the IRE is fully immersed) in the presence of liquid water when compared to high humidity conditions (RH~100%). It should be noted that for all humidity measurements condensed water was not visibly observed on the surface of the IRE.

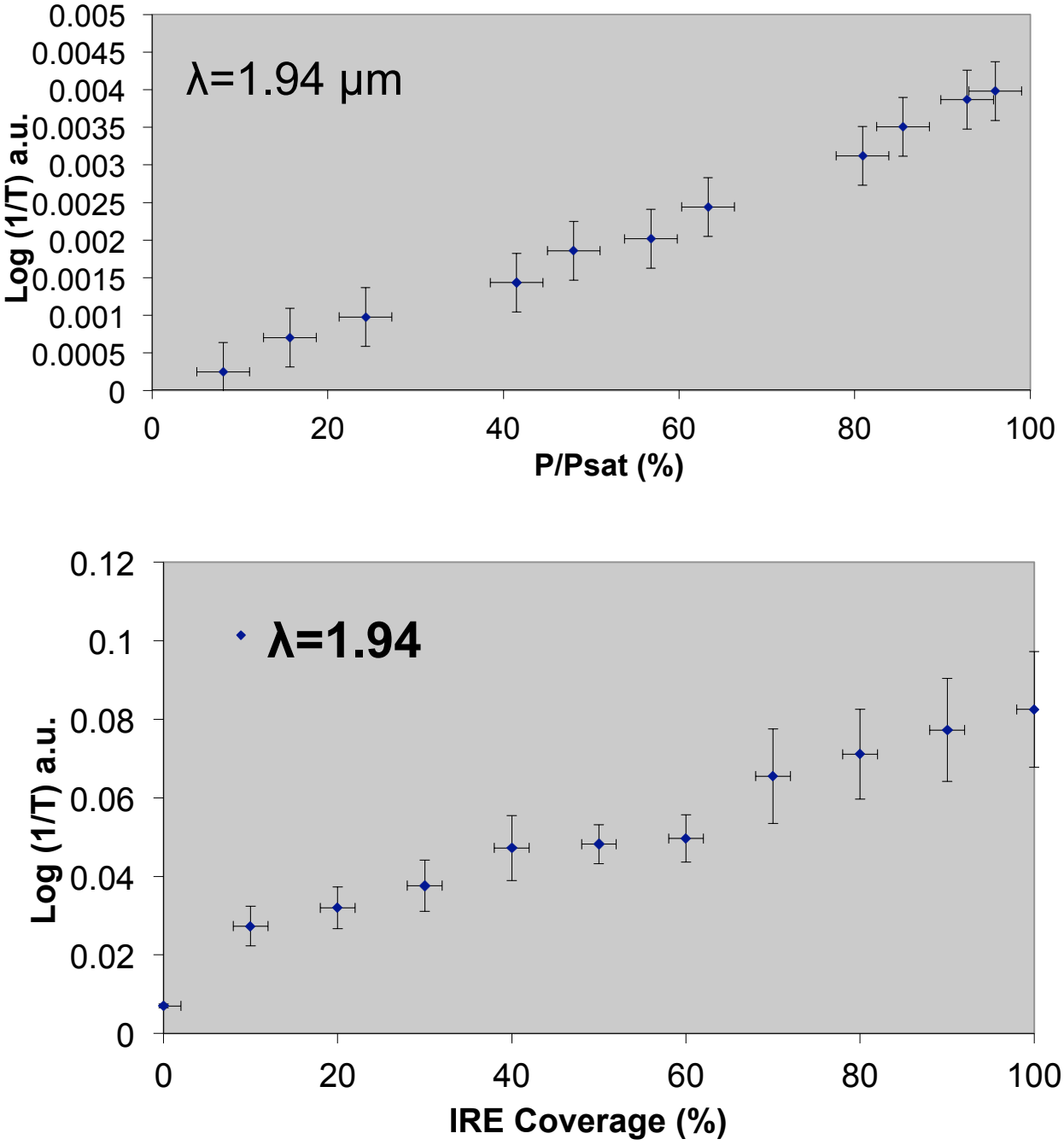

Figure 4.7 Comparison of peak absorbance of adsorbed water with respect to changes in relative humidity (top figure) to peak absorbance of liquid water with respect to IRE coverage (bottom figure). Measurements displayed were of the water absorption band at λ=1.94μm (IRE length = 5cm)

Ice Measurements

Spectral results show a shift to longer wavelengths in the presence of ice and weaker absorbance (relative to liquid water) at λ=1.94 and λ=1.45 μm. The presence of ice is indicated in Fig 4.8 by a shift in wavelength from 1.94 to 1.97 μm and 1.45 to 1.48 μm. This shift was present in all ice measurements. Distinguishing between liquid and solid phases of water is an important feature optical sensors can provide for analysis of soil analogs at Mars-relevant temperatures (170-250 K). This is also relevant for studies of the stability of brine solutions due to concentrations of perchlorate salts [Chevrier et al, 2009].

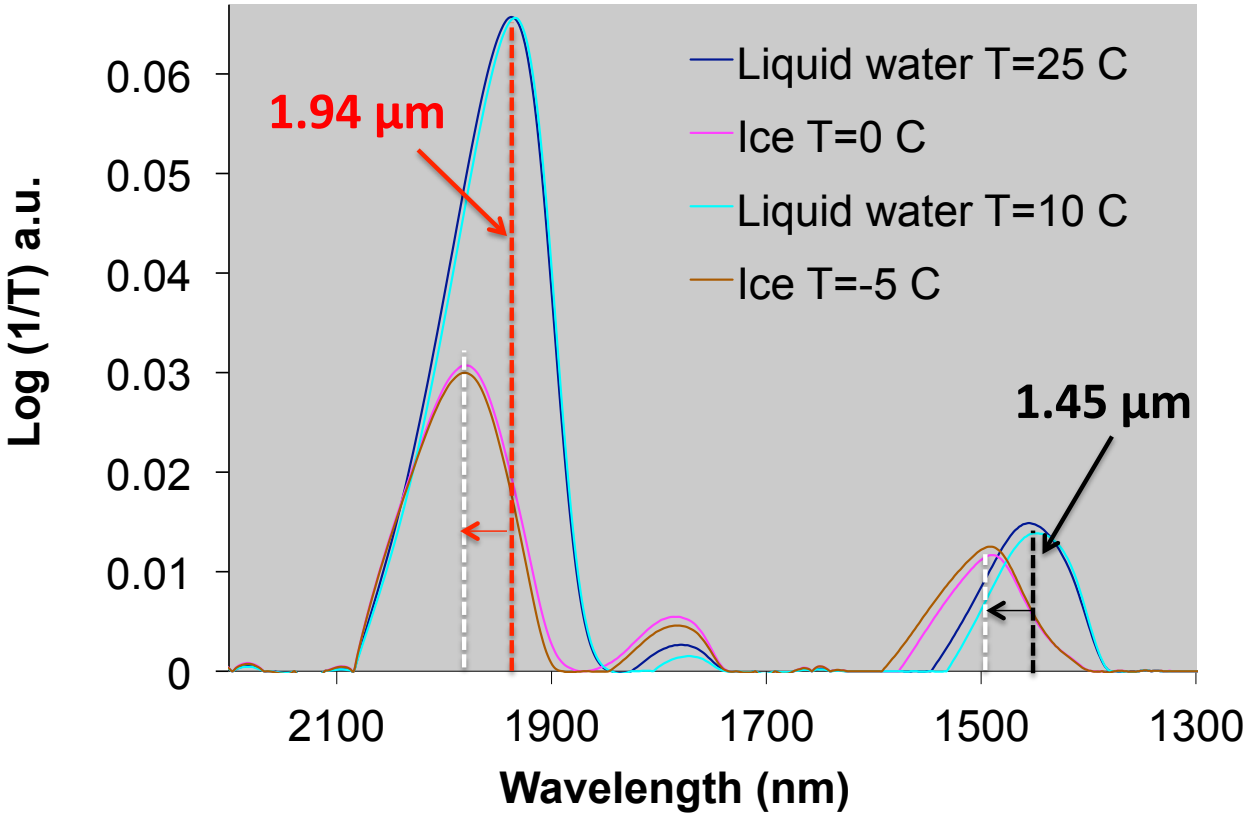

Fig 4.8: Near-infrared spectra showing spectral shift in the presence of ice. Black arrows indicate shifting to longer wavelengths. The IRE was completely immersed for these measurements, IRE length = 5cm.

Error bars plotted in Figs 4.3, 4.4, 4.6, and 4.7 were calculated using a root-mean square deviation from average peak absorbance values. Deviations from plotted measurements on the x-axis were attributed to IRE water immersion depth measurement error (±1mm) or error in the relative humidity sensor (±3%). Peak absorbance values (y-axis) were averaged for each data set and error bars represent deviations from average. Absorbance error is attributed to fluctuations in the performance of the spectrometer and alignment deviations in regard to the optical coupler.

Ch. 5 Conclusions

This thesis has demonstrated that near-infrared absorption due to the evanescent field of optical sensors is a viable means to investigate the presence of various phases of water. Measured results of the technique described in this work agree well with theoretical calculations of absorbance in liquid water. Therefore, absorbance as a function of evanescent wave coefficient and path length can be used for quantitative analysis of liquid water within the evanescent field. Another important feature of this thesis is the analysis of adsorbed water with optical sensors. Other authors have observed adsorbed water using Attenuated Total Reflection (ATR) crystals [Asay & Kim, 2005] and liquid water in heterogeneous media [Zhang et al., 2009], but direct analysis of adsorbed water and the development of optical sensors for continuous localized measurements in subsurface environments has not been performed before.

Future work should implement intrinsic optical sensor systems to investigate evanescent wave absorption in heterogeneous particulate media. Soil media analogous to non-terrestrial environments, such as those observed on the surface of Mars, have been developed and are easily integrated in the facility described in this thesis. The methods employed in this work could be effective in analysis of water content in void spaces between particle grains, which in turn could provide insight into thermal properties of the subsurface of Mars. Other experiments should include analysis of water absorption in the mid-infrared at the fundamental vibrations of water. This region can provide insight to the structure of adsorption layers due to shifting in the antisymmetric and symmetric stretch absorption bands (ν_1 and ν_3) [Asay & Kim, 2005]. These bands are significant because they identify regions of adsorbed water that behave similarly to liquid water. Regions of this "liquid-like" water could be utilized by microbes capable of undergoing metabolic processes in thin films of water. The efficiency of these films as transport

mechanisms varies with adlayer thickness [Rivkina et al., 2000]. Optical cables that transmit in the mid-infrared are composed of chalcogenide, silver halide, fluoride, and sapphire glass [Saito & Kikuchi, 1997]. Preliminary work integrating mid-infrared optical cables with the facility described in this thesis is currently in progress.

References

Anderson, D. M. and Morgenstern, N. R. (1973). "Physics, chemistry, and mechanics of frozen ground: a review," Proceedings of Permafrost: Second International Conference. National Academy of Sciences, Washington, D.C. 257–288.

Asay, D. and Kim, S. (2005). "Evolution of the Adsorbed Water Layer Structure on Silicon Oxide at Room Temperature," *Journal of Physical Chemistry*, 109, 16760-16763.

Bogdan, A. (2000). "Fumed silica as a host for study of large surface-to-volume ratio problems in finely divided aqueous systems: Implications for the atmosphere," Adsorption on Silica Surfaces (Marcel Dekker, Inc.; New York, 2000) 689-745.

Carter, M.R. and Gregorich, E.G. Soil Sampling and Methods of Analysis. Boca Raton: Taylor and Francis Group, 2006.

Chen, Z., Lu, C. (2005). "Humidity Sensors: A Review of Materials and Mechanisms," *Sensor Letters*, 3, 274–295.

Chevrier, V. F., et al. (2009). "Stability of perchlorate hydrates and their liquid solutions at the Phoenix landing site, Mars," *Geophysical Research Letters*, 10.1029/2009GL037497.

Christner, B. C. et al. (2000). "Recovery and Identification of Viable Bacteria Immured in Glacial Ice," *Icarus* 144, 479–485.

Curcio, J. A. and Petty, C. C. (1951). "The Near Infrared Absorption Spectrum of Liquid Water," *Journal of the Optical Society of America*, 41(5), 302-304.

Degrandpre, M. D., Burgess, L. (1990). "A fiber-optic FT-NIR evanescent field absorbance sensor," *Applied Spectroscopy*, 44(2), 273.

Feldman, W. C., et al. (2004). "Global Distribution of Near-Surface Hydrogen on Mars," *Journal of Geophysical Research*, **109**, E09006, doi:10.1029/2003JE002160, 2004.

Mohlmann, D. (2003) "Water in the upper martian surface at mid- and low-latitudes: Presence, state, and consequences," *Icarus*, 168, 318-323.

Harrick, N.J. Internal Reflectance Spectroscopy. New York: John Wiley & Sons, 1967.

Harrington, James A. Infrared Fibers and their applications. Bellingham: SPIE, 2004.

Hudson, T. L. et al. (2009). "Laboratory experiments and models of diffusive emplacement of ground ice on Mars," *Journal of Geophysical Research*, **114**, e01002, doi:10.1029/2008JE003149, 2009.

Inaba, H. (1979). "Optical-fibre network system for air-pollution monitoring over a wide area by optical absorption method," *Electronics Letters*, 15 (23), 749.

Jakosky, B. M. et al. (2005) "Mars low-latitude neutron distribution: Possible remnant near-surface water ice and a mechanism for its recent emplacement," *Icarus*, 175, 58-67.

Janchen, J. et al. (2006). "Investigation of the water sorption properties of Mars-relevant micro- and mesoporous minerals," *Icarus*, 180, 353-358.

Littlejohn, D. et al. (1999). Bent silica fiber evanescent absorption sensors for near-infrared spectroscopy. *Applied Spectroscopy*, 53(7), 845-849.

Ostroumov, V. E. and Siegert, C. (1996). Exobiological aspects of mass transfer in microzones of permafrost deposits. *Advances in Space Research*. 18(12), 79–86.

Pikuta, E V.. and Hoover, R. B (2003) "Psychrophiles and Astrobiology: Microbial Life of Frozen Worlds," Instruments, Methods, and Missions for Astrobiology VI, Proceedings of SPIE Vol. 4939.

Piqueux, S. and Christensen, P.R. (2009) "A model of thermal conductivity for planetary soils: 1. Theory for unconsolidated soils" *Journal of Geophysical Research*, 114, E09005, doi:10.1029/2008JE003308.

Rivkina et al. (2000). Metabolic Activity of permafrost Bacteria below the freezing point. *Applied and Environmental* Microbiology, 66(8), 3230-3233.

Saito, M and Kikuchi K. (1997). "Infrared Optical Fiber Sensors," *Optical Review,* 4(5), 527.538.

Santamarina, J.C., and Fam, M. J. (1997), "Dielectric Permittivity of Soils Mixed with Organic and Inorganic Fluids (0.02 GHz to 1.30 GHz)," *Journal of Environmental & Engineering Geophysics,* 2, 37.

Schneider, M. "Experimental Investigation of Water Vapor Adsorption by Molecular Sieve Zeolite 3A under Simulated Martian Atmospheric Conditions," MS thesis, Department of Aeronautics & Astronautics, University of Washington, Seattle, WA, 2003.

Schneider, M. A., and Bruckner, A. P., "Extraction of Water from the Martian Atmosphere," *Space Technology & Applications International Forum – STAIF-2003*, Albuquerque, NM, Feb. 2-5, 2003, M.S. El-Genk, ed., American Institute of Physics Conference Proceedings, Volume 654, pp. 1124-1132.

Siegler et al. 2012, "Measurements of thermal properties of icy Mars regolith analogs," *Journal of Geophysical Research*, E03001, doi:10.1029/2011JE003938.

Simhony et al. (1986). "Novel attenuated total internal reflectance spectroscopic cell using infrared fibers for aqueous solutions," *Applied Physics Letters*, 49, 253.

Smith, M. D., "The annual cycle of water vapor on Mars as observed by the Thermal Emission Spectrometer," *Journal of Geophysical Research*, **107** (E11), 5115, doi:10.1029/2001JE001522, 2002.

Rettner, C.T et al. (1996). "Chemical Dynamics at the Gas-Surface Interface," *Journal of Physical Chemistry,* 100, 13021-13033.

Ruthven, D. M. Principles of adsorption and adsorption processes. New York: John Wiley & Sons, 1984.

Warren, S.G. and Brandt, R. E. (2008) "Optical constants of ice from the ultraviolet to the microwave: A revised compilation," *Journal of Geophysical Research*, 113, d14220, doi:10.1029/2007jd009744.

Wood, S. E. (2011) "A general analytic model for the thermal conductivity of loose, indurated, or icy planetary regolith," Proceedings: Lunar Planetary Science Conference, 42nd, 2795.

Xiong, F. B. and Sisler, D. (2010) "Determination of low-level water content in ethanol by fiber-optic evanescent absorption sensor," *Optics Communication* 1326-1330.

Zent, A. P. et al. (2009), "Thermal and Electrical Conductivity Probe (TECP) for Phoenix *Journal of Geophysical Research*, 114, E00A27, doi:10.1029/2007JE003052.

Zhang et al. (2009), "Sapphire Fiber Evanescent Wave Absorption in Turbid Media," *Applied Spectroscopy*, 932-935.

Appendix

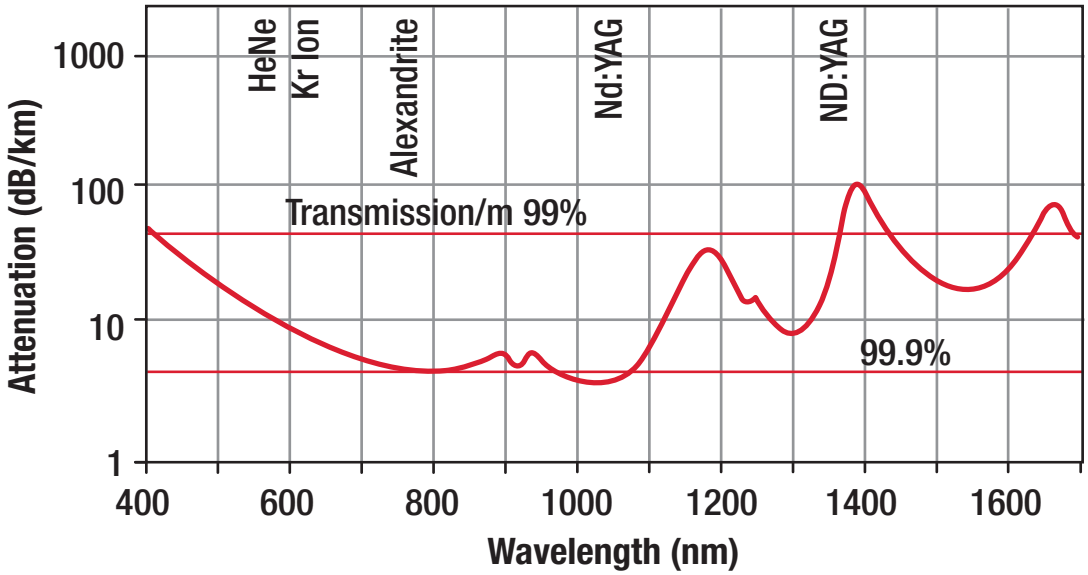

Fig. A.1: Transmission of SiO_2 near-infrared optical cable [Courtesy of Thorlabs, Inc.]

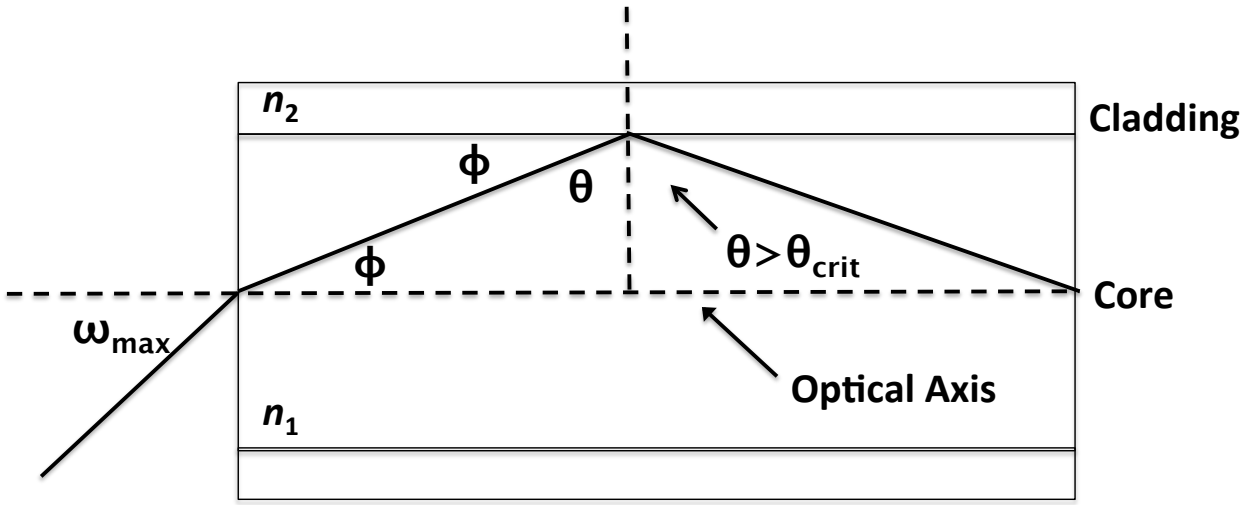

Fig A.2: Total Internal Reflection at core-cladding interface

λ (μm)	RH=8.1%	RH=15.7%	RH=24.3%	RH=41.5%	RH=48.0%	RH=56.8%	RH=63.3%	RH=80.9%	RH=85.5%	RH=92.8%	RH=96.0%
1.3877517	-2.6491E-05	1.21604E-05	7.81737E-06	5.64586E-06	9.12028E-06	2.17148E-06	0	5.64586E-06	2.9533E-05	3.95226E-05	2.73614E-05
1.3907432	0	5.51589E-05	4.60377E-05	4.82094E-05	5.34215E-05	3.99569E-05	4.7775E-05	5.21185E-05	0.000105112	0.000121185	0.000107718
1.3937282	4.34297E-06	9.33834E-05	7.42707E-05	8.33925E-05	8.86051E-05	6.55834E-05	8.86051E-05	8.1655E-05	0.000161588	0.000176359	0.000167236
1.3967261	1.38976E-05	0.000117275	8.7302E-05	0.000102506	0.000105981	7.20989E-05	0.000116407	9.2949E-05	0.000194608	0.000204601	0.000202428
1.3997368	2.60585E-05	0.000143341	0.00010685	0.000128136	0.00012857	8.38269E-05	0.000154636	0.00011771	0.000238493	0.000245011	0.000252398
1.4027803	4.3866E-05	0.00018809	0.000152464	0.000180704	0.000178532	0.000123792	0.000225457	0.000178097	0.000319758	0.000328451	0.000346705
1.4058173	6.81896E-05	0.000253702	0.000225023	0.000262828	0.000258048	0.000195042	0.000326278	0.000269781	0.000435816	0.000454075	0.000484509
1.4088674	9.42521E-05	0.000328885	0.000309762	0.000357572	0.00035279	0.000281949	0.000439294	0.000374089	0.00056669	0.00060061	0.000643232
1.4119508	0.000115972	0.00040017	0.000390172	0.00044538	0.000443206	0.000366265	0.000544947	0.000469726	0.000690208	0.000740234	0.000798098
1.4150276	0.000128136	0.000458423	0.000455814	0.000514075	0.000516249	0.000432338	0.000629749	0.000541033	0.000788961	0.000848571	0.000925599
1.4181179	0.000129439	0.000503639	0.000504074	0.000559732	0.000565385	0.000472335	0.000686728	0.00058017	0.000854228	0.000914283	0.001013522
1.4212419	0.000122054	0.000539294	0.000535815	0.000585824	0.000591477	0.000484509	0.000715438	0.000589738	0.00088643	0.000940832	0.001060973
1.4243594	0.000109456	0.000568864	0.000554514	0.000595391	0.000598871	0.000474074	0.000721093	0.000576691	0.000890782	0.000940832	0.001073599
1.4274906	9.2949E-05	0.000588868	0.000561471	0.000589738	0.000591912	0.000447989	0.000706738	0.000544947	0.000871635	0.000921682	0.00105662
1.4306356	6.94927E-05	0.000593217	0.000553644	0.000568429	0.000572343	0.000410168	0.000674549	0.000495813	0.000832036	0.000885995	0.001013087
1.4338151	3.77853E-05	0.000579301	0.000531032	0.000533641	0.000541468	0.000361049	0.000628009	0.000432338	0.000777649	0.000835517	0.000951277
1.4369881	0	0.000551905	0.000499291	0.0004919	0.00050277	0.000304113	0.000574952	0.000361918	0.000715873	0.000774603	0.000880338
1.4401751	-5.6458E-06	0.000520162	0.000467118	0.000450162	0.000461031	0.000242838	0.00052451	0.000289336	0.000653671	0.000709348	0.000808105
1.4433972	-8.2515E-06	0.000489726	0.000440598	0.000411472	0.000417992	0.000182008	0.00048103	0.000220678	0.000596261	0.000645407	0.000740234
1.4466128	-8.2515E-06	0.000463205	0.000419297	0.000378435	0.000376697	0.000126833	0.000444511	0.000158981	0.000548861	0.000588433	0.000678898
1.4498427	-6.9487E-06	0.000442772	0.000401039	0.000351486	0.000339317	7.99175E-05	0.000412776	0.000104243	0.000511031	0.000541468	0.0006254
1.4531082	-4.3429E-06	0.000429295	0.000383217	0.000330624	0.000307155	3.99569E-05	0.000382347	5.38559E-05	0.000478422	0.00050103	0.000577561
1.4563672	0	0.000420166	0.000363222	0.000308459	0.000277168	0	0.000348879	0	0.000441902	0.000457118	0.000528423
1.4596409	9.12028E-06	0.000408429	0.000339317	0.000276734	0.000242838	1.82408E-05	0.000307155	2.43212E-05	0.000393649	0.000401039	0.000468857
1.4629294	1.52006E-05	0.000389737	0.000310197	0.000230237	0.000200256	2.56241E-05	0.000254571	3.17047E-05	0.00032932	0.000328885	0.000393214
1.4662542	1.60692E-05	0.000362353	0.000276299	0.00017158	0.000151161	2.30182E-05	0.000192435	2.51898E-05	0.00025066	0.000245446	0.00030107
1.4695725	1.12918E-05	0.000328016	0.000238493	0.000108153	9.8596E-05	1.3029E-05	0.00012466	1.12918E-05	0.000164194	0.000157678	0.000198952
1.4729059	3.90867E-06	0.000291944	0.000199821	4.9078E-05	4.69063E-05	3.04007E-06	5.86337E-05	4.34295E-07	7.77457E-05	7.38363E-05	9.59897E-05
1.4762762	0	0.000260655	0.000165498	0	0	0	0	0	0	0	0
1.4796402	-6.0801E-06	0.000238059	0.000138562	-4.3429E-07	-1.3029E-06	-2.6058E-06	-4.3429E-06	-7.3829E-06	-5.2115E-06	3.90867E-06	-4.3429E-06
1.4830194	-4.3429E-06	0.000223285	0.00011771	3.90867E-06	1.73718E-06	3.47437E-06	4.34295E-07	-4.7772E-06	-2.6058E-06	1.21604E-05	-1.7372E-06
1.4864363	8.6859E-07	0.000211118	9.68585E-05	7.81737E-06	4.77727E-06	1.12918E-05	7.38307E-06	1.73718E-06	2.17148E-06	1.82408E-05	2.60577E-06
1.4898467	4.34297E-06	0.000197649	7.16645E-05	9.12028E-06	5.64586E-06	1.38976E-05	1.17261E-05	6.08017E-06	5.21157E-06	1.82408E-05	5.21157E-06
1.4932728	4.34297E-06	0.000179401	3.90883E-05	6.94877E-06	4.34297E-06	9.98889E-06	9.12028E-06	5.64586E-06	4.34297E-06	1.08575E-05	3.90867E-06
1.4967371	0	0.00015594	0	0	0	0	0	0	0	0	0
1.500195	-3.4743E-06	0.000129005	-5.6458E-06	0	3.47437E-06	-4.7772E-06	-1.7372E-06	-8.6859E-07	-2.6058E-06	-3.4743E-06	-1.3029E-06
1.503669	-5.6458E-06	0.000101637	-1.0857E-05	-3.4743E-06	6.08017E-06	-8.2515E-06	-2.1715E-06	-2.1715E-06	-4.7772E-06	-5.2115E-06	-1.7372E-06
1.507159	-4.3429E-06	7.60082E-05	-1.0857E-05	-5.6458E-06	8.25167E-06	-7.3829E-06	0	-2.1715E-06	-4.7772E-06	-3.4743E-06	0
1.5106881	-8.6859E-07	5.12498E-05	-7.3829E-06	-5.2115E-06	8.25167E-06	-4.3429E-06	3.04007E-06	-8.6859E-07	-3.0401E-06	0	2.17148E-06
1.5142109	1.73718E-06	2.64928E-05	-3.0401E-06	-2.1715E-06	5.21157E-06	-1.3029E-06	3.47437E-06	4.34295E-07	-4.3429E-07	2.17148E-06	3.47437E-06
1.5177501	0	0	0	0	0	0	0	0	0	0	0
1.521329	6.51447E-06	6.08017E-06	4.34297E-06	6.08017E-06	3.04007E-06	8.68598E-06	2.17148E-06	4.77727E-06	6.51447E-06	3.04007E-06	5.21157E-06
1.5249016	9.12028E-06	9.55458E-06	6.51447E-06	9.55458E-06	4.77727E-06	1.3029E-05	3.47437E-06	6.51447E-06	8.25167E-06	3.04007E-06	6.08017E-06
1.5284911	7.81737E-06	1.12918E-05	6.08017E-06	1.17261E-05	5.64586E-06	1.34633E-05	4.34297E-06	6.51447E-06	7.81737E-06	3.04007E-06	5.21157E-06
1.5321209	5.21157E-06	1.08575E-05	5.21157E-06	1.21604E-05	6.08017E-06	1.04232E-05	4.77727E-06	5.21157E-06	6.51447E-06	3.47437E-06	4.34297E-06
1.5357445	2.60577E-06	7.38307E-06	3.47437E-06	8.68598E-06	4.34297E-06	5.64586E-06	3.90867E-06	2.60577E-06	3.90867E-06	3.04007E-06	2.60577E-06
1.5393852	0	0	0	0	0	0	0	0	0	0	0
1.5430432	-4.3429E-06	-6.0801E-06	2.17148E-06	-7.3829E-06	-4.3429E-07	1.73718E-06	4.34295E-07	2.17148E-06	-1.7372E-06	-3.0401E-06	-3.4743E-06
1.5467426	-6.0801E-06	-1.1726E-05	2.17148E-06	-1.3463E-05	-2.6058E-06	3.47437E-06	-4.3429E-07	4.77727E-06	-4.3429E-06	-5.2115E-06	-5.6458E-06
1.5504357	-5.2115E-06	-1.3029E-05	8.6859E-07	-1.6069E-05	-5.2115E-06	3.47437E-06	-1.3029E-06	6.08017E-06	-7.3829E-06	-6.5144E-06	-6.5144E-06
1.5541465	-3.0401E-06	-1.0423E-05	-1.7372E-06	-1.4331E-05	-6.5144E-06	2.17148E-06	-1.7372E-06	5.21157E-06	-8.6858E-06	-6.5144E-06	-5.6458E-06
1.5578993	-4.3429E-07	-5.2115E-06	-2.1715E-06	-8.6858E-06	-5.2115E-06	0	-1.7372E-06	3.04007E-06	-6.0801E-06	-4.3429E-06	-3.0401E-06
1.561646	0	0	0	0	0	0	0	0	0	0	0
1.5654107	-1.3029E-06	3.04007E-06	1.30289E-06	6.51447E-06	1.30289E-06	-2.6058E-06	-3.4743E-06	-3.9086E-06	3.90867E-06	1.73718E-06	-4.3429E-07
1.5692182	-4.7772E-06	2.17148E-06	1.73718E-06	7.38307E-06	3.47437E-06	-3.4743E-06	-6.5144E-06	-7.8172E-06	3.90867E-06	2.60577E-06	-3.4743E-06
1.5730196	-7.8172E-06	-1.7372E-06	8.6859E-07	3.47437E-06	4.34297E-06	-3.0401E-06	-8.6858E-06	-9.9887E-06	4.34295E-07	2.60577E-06	-6.9487E-06
1.5768394	-7.8172E-06	-4.3429E-06	0	-1.3029E-06	3.90867E-06	-2.1715E-06	-7.8172E-06	-8.2515E-06	-3.4743E-06	1.73718E-06	-8.2515E-06
1.5806778	-4.3429E-06	-3.0401E-06	4.34295E-07	-2.6058E-06	2.60577E-06	-4.3429E-07	-3.4743E-06	-3.9086E-06	-3.4743E-06	1.30289E-06	-5.2115E-06
1.58456	0	0	0	0	0	0	0	0	0	0	0
1.5884362	5.21157E-06	6.51447E-06	4.77727E-06	8.68598E-06	6.08017E-06	8.68598E-06	8.25167E-06	7.81737E-06	1.12918E-05	4.34297E-06	1.4332E-05
1.5923313	9.55458E-06	1.17261E-05	6.08017E-06	1.56349E-05	1.12918E-05	1.3029E-05	1.21604E-05	1.3029E-05	1.9978E-05	7.38307E-06	2.1281E-05
1.5962711	1.3029E-05	1.38976E-05	5.64586E-06	1.82408E-05	1.47663E-05	1.3029E-05	1.21604E-05	1.52006E-05	2.25839E-05	9.55458E-06	1.95437E-05
1.6002048	1.21604E-05	1.3029E-05	4.34297E-06	1.60692E-05	1.38976E-05	9.55458E-06	9.55458E-06	1.38976E-05	1.82408E-05	9.98889E-06	1.3029E-05
1.604158	6.94877E-06	7.38307E-06	2.17148E-06	9.12028E-06	7.81737E-06	3.90867E-06	5.21157E-06	8.25167E-06	9.12028E-06	7.38307E-06	5.21157E-06
1.6081566	0	0	0	0	0	0	0	0	0	0	0
1.6121492	4.34295E-07	-2.6058E-06	3.47437E-06	5.64586E-06	4.34297E-06	3.47437E-06	5.21157E-06	8.6859E-07	2.60577E-06	3.47437E-06	4.34297E-06
1.6161616	1.73718E-06	-2.6058E-06	6.51447E-06	1.17261E-05	8.68598E-06	9.12028E-06	9.55458E-06	4.34297E-06	8.25167E-06	5.21157E-06	9.55458E-06
1.6201941	2.60577E-06	0	8.68598E-06	1.56349E-05	1.12918E-05	1.38976E-05	1.12918E-05	9.55458E-06	1.34633E-05	6.51447E-06	1.21604E-05
1.6242731	3.04007E-06	3.04007E-06	8.68598E-06	1.47663E-05	1.04232E-05	1.4332E-05	9.98889E-06	1.12918E-05	1.4332E-05	6.94877E-06	1.17261E-05
1.6283463	2.17148E-06	3.90867E-06	6.08017E-06	9.55458E-06	6.51447E-06	9.98889E-06	6.08017E-06	8.25167E-06	9.12028E-06	5.21157E-06	7.38307E-06
1.6324398	0	0	0	0	0	0	0	0	0	0	0
1.6365809	1.9978E-05	3.3442E-05	3.73509E-05	4.56033E-05	5.6462E-05	5.25528E-05	5.60276E-05	5.03811E-05	5.25528E-05	5.47246E-05	6.55834E-05
1.640716	3.73509E-05	5.99368E-05	6.94927E-05	8.42613E-05	0.000102506	9.64241E-05	0.000101637	9.33834E-05	9.77273E-05	9.98992E-05	0.000120316
1.6448721	4.86437E-05	7.47051E-05	8.99083E-05	0.000108153	0.00012857	0.000122923	0.000128136	0.000120316	0.000125964	0.000128136	0.000153767
1.6490765	4.9078E-05	7.25332E-05	8.99083E-05	0.000107718	0.00012466	0.000121185	0.000125095	0.000121619	0.000125964	0.00012857	0.000153767
1.6532751	3.3442E-05	4.86437E-05	6.16742E-05	7.38363E-05	8.38269E-05	8.20894E-05	8.46957E-05	8.46957E-05	8.68676E-05	8.99083E-05	0.000105981
1.6574952	0	0	0	0	0	0	0	0	0	0	0
1.6617368	2.73614E-05	3.73509E-05	4.43003E-05	5.55933E-05	6.03711E-05	5.55933E-05	6.42803E-05	6.42803E-05	6.55834E-05	7.47051E-05	7.99175E-05
1.666028	3.56136E-05	4.95124E-05	5.7765E-05	6.9927E-05	7.47051E-05	6.86239E-05	8.07863E-05	7.73113E-05	7.86144E-05	9.03426E-05	9.77273E-05
1.6703135	3.04017E-05	4.25629E-05	4.7775E-05	5.47246E-05	5.51589E-05	5.08154E-05	6.21086E-05	5.42902E-05	5.38559E-05	6.42803E-05	7.07958E-05
1.6746211	1.95437E-05	2.56241E-05	2.82301E-05	2.86644E-05	2.47555E-05	2.25839E-05	3.04017E-05	2.1281E-05	1.86751E-05	2.43212E-05	3.04017E-05
1.6789792	8.25167E-06	9.55458E-06	9.98889E-06	8.25167E-06	3.47437E-06	3.04007E-06	6.94877E-06	8.6859E-07	-2.1715E-06	-4.3429E-07	3.90867E-06
1.6833317	0	0	0	0	0	0	0	0	0	0	0
1.6877067	-3.4742E-05	-4.3427E-05	-5.7757E-05	-6.8179E-05	-6.9047E-05	-6.5139E-05	-6.9482E-05	-6.6876E-05	-6.21E-05	-7.035E-05	-8.4679E-05
1.6921333	-6.1231E-05	-7.5561E-05	-0.00010422	-0.00012549	-0.00012983	-0.00012115	-0.0001294	-0.00013201	-0.00012289	-0.00013678	-0.00016543
1.6965543	-7.5561E-05	-9.4666E-05	-0.00013331	-0.0001637	-0.00017499	-0.0001624	-0.00017368	-0.00018497	-0.00017542	-0.00019278	-0.00023055

Table A.3 Absorbance data Fig 4.2 (1 of 2)

λ (μm)	RH=8.1%	RH=15.7%	RH=24.3%	RH=41.5%	RH=48.0%	RH=56.8%	RH=63.3%	RH=80.9%	RH=85.5%	RH=92.8%	RH=96.0%
1.7009985	-7.2521E-05	-9.3797E-05	-0.00013244	-0.00016587	-0.0001815	-0.00016934	-0.00018019	-0.00019669	-0.00018975	-0.00020667	-0.00024357
1.705466	-4.8204E-05	-6.4271E-05	-8.9455E-05	-0.00011247	-0.00012593	-0.00011811	-0.00012549	-0.00013722	-0.00013418	-0.00014546	-0.00016891
1.7099863	0	0	0	0	0	0	0	0	0	0	0
1.7145013	-2.0411E-05	-3.1702E-05	-2.8662E-05	-3.5611E-05	-3.8216E-05	-3.3439E-05	-4.6033E-05	-3.1268E-05	-3.7782E-05	-3.6045E-05	-4.0388E-05
1.7190401	-2.9531E-05	-4.3427E-05	-4.0388E-05	-4.9073E-05	-4.9073E-05	-4.2125E-05	-6.0363E-05	-3.6045E-05	-4.7336E-05	-4.3862E-05	-5.0809E-05
1.7236327	-3.1268E-05	-4.3862E-05	-4.3862E-05	-5.2546E-05	-4.9941E-05	-4.3862E-05	-6.0797E-05	-3.5611E-05	-4.8204E-05	-4.5164E-05	-5.4283E-05
1.7282201	-2.3451E-05	-3.2571E-05	-3.5176E-05	-4.1256E-05	-3.9085E-05	-3.6913E-05	-4.5599E-05	-3.04E-05	-3.865E-05	-3.7782E-05	-4.6033E-05
1.732832	0	0	0	0	0	0	0	0	0	0	0
1.7374987	3.25733E-05	7.16645E-05	7.42707E-05	7.818E-05	7.51394E-05	7.68769E-05	8.64332E-05	7.86144E-05	8.90395E-05	9.2949E-05	0.000103809
1.7421603	8.38269E-05	0.00018027	0.000189828	0.000209815	0.000213291	0.000215464	0.000234148	0.000229368	0.000245446	0.000263262	0.000294552
1.7468469	0.000147251	0.000315847	0.00033497	0.000384086	0.000404082	0.000402343	0.000432773	0.000441902	0.000460162	0.000498856	0.000558427
1.7515589	0.000215029	0.000458857	0.000490161	0.000576691	0.000615397	0.000606699	0.000652801	0.000681508	0.000702388	0.000762421	0.000853358
1.7563272	0.000280645	0.000591477	0.000637143	0.000761551	0.000814631	0.000799403	0.000862931	0.000907755	0.000936044	0.001011781	0.00113412
1.7610905	0.000339317	0.000704128	0.000765467	0.000920376	0.00098131	0.000962594	0.001041818	0.001094933	0.001135426	0.001220779	0.001369315
1.7658797	0.00038626	0.000794617	0.000867718	0.001044866	0.001108865	0.001091014	0.001182019	0.001237764	0.001292209	0.001382386	0.001550154
1.7707264	0.000417558	0.000861191	0.000940832	0.001132813	0.001198568	0.001185068	0.001282627	0.001341869	0.001407656	0.00150265	0.001681364
1.7755682	0.000434512	0.000904708	0.000985228	0.001186374	0.001256057	0.001247782	0.001348404	0.001415063	0.001486525	0.001587639	0.00177293
1.7804366	0.000439729	0.000925163	0.001005251	0.001209891	0.00128524	0.001281755	0.001383693	0.001459072	0.001531849	0.001640384	0.00182875
1.7853636	0.00043712	0.000923858	0.001003945	0.001205971	0.001288289	0.001286982	0.001388921	0.00146953	0.001541873	0.001656514	0.001844887
1.7902859	0.000425383	0.000899051	0.000979134	0.00117331	0.001261719	0.00125867	0.00135886	0.001439899	0.001513545	0.001630794	0.001813922
1.7952354	0.000401908	0.000847266	0.000925163	0.001105818	0.001197697	0.001189858	0.001286547	0.001363216	0.001440335	0.001554949	0.001724964
1.8002448	0.000364526	0.000765467	0.000837258	0.000998722	0.001087966	0.00107447	0.001164601	0.001234716	0.001313554	0.001419856	0.001569332
1.8052497	0.000313239	0.000651931	0.000712828	0.000849442	0.00092908	0.000912107	0.000991322	0.001052266	0.001127588	0.001219472	0.001343176
1.8102824	0.000248922	0.000507552	0.000556253	0.0006615	0.000725008	0.000708043	0.000771558	0.000820288	0.00088469	0.0009565	0.00105096
1.8153433	0.000171146	0.000339751	0.000374958	0.000444511	0.000487987	0.000474943	0.000518423	0.000552339	0.000598871	0.000647146	0.000710653
1.8204657	8.55644E-05	0.00016376	0.000183311	0.000216333	0.000238059	0.000231541	0.000252398	0.00027065	0.000294117	0.000317151	0.000349313
1.8255837	0	0	0	0	0	0	0	0	0	0	0
1.8307306	-4.4296E-05	-9.8574E-05	-0.00010726	-0.00012593	-0.00014069	-0.00013765	-0.00015328	-0.00016847	-0.00019018	-0.00020407	-0.00021883
1.8359404	-6.5574E-05	-0.00014156	-0.00015849	-0.00018454	-0.00020928	-0.00020581	-0.00023055	-0.00025616	-0.00029131	-0.00031345	-0.00033688
1.8411459	-6.0363E-05	-0.00012245	-0.00014112	-0.00016413	-0.00019148	-0.00018671	-0.00021319	-0.00024097	-0.00027569	-0.00029956	-0.00032256
1.8463811	-3.6913E-05	-6.21E-05	-7.6863E-05	-8.9455E-05	-0.00011117	-0.00010465	-0.00012636	-0.00014546	-0.00016847	-0.00018844	-0.0002019
1.8516804	-1.2594E-05	-9.1201E-06	-1.6069E-05	-1.9543E-05	-3.0834E-05	-2.5188E-05	-3.6913E-05	-4.3427E-05	-5.1678E-05	-6.2534E-05	-6.6442E-05
1.8569757	0	0	0	0	0	0	0	0	0	0	0
1.8623014	-8.2515E-06	-1.9543E-05	-2.2583E-05	-2.6925E-05	-3.04E-05	-3.2571E-05	-3.4308E-05	-3.9519E-05	-4.2993E-05	-4.5164E-05	-4.9941E-05
1.8676578	0	0	0	0	0	0	0	0	0	0	0
1.8730801	8.25167E-06	5.68963E-05	7.77457E-05	9.55553E-05	0.000142906	0.000122923	0.000165932	0.000198952	0.000221547	0.000240231	0.000221981
1.8784987	5.21185E-05	0.000221112	0.000278907	0.000345401	0.000450162	0.000431034	0.00052451	0.000631489	0.000700213	0.00074937	0.000736754
1.8839488	0.000117275	0.000427556	0.000533207	0.000675854	0.000842479	0.000842914	0.000989146	0.001195084	0.001320959	0.001408091	0.001415063
1.8894662	0.000182442	0.000596261	0.000754155	0.000987404	0.00121294	0.001245168	0.001442078	0.001748074	0.001926454	0.002056032	0.002082214
1.8949802	0.000229803	0.000685423	0.000894264	0.001215988	0.001493062	0.001564538	0.001806508	0.002203982	0.002423599	0.002595266	0.002638521
1.9005264	0.000250226	0.000704563	0.000958241	0.001351454	0.001670901	0.001782523	0.002064759	0.002548083	0.00280153	0.003015327	0.003076556
1.9061416	0.000242838	0.000691078	0.000978264	0.001415063	0.001770313	0.001915984	0.002235411	0.002798907	0.003086179	0.003341691	0.003426165
1.9117535	0.000219374	0.000679333	0.000986534	0.00143467	0.001820464	0.001987966	0.002341939	0.002972909	0.003294427	0.003589471	0.003699397
1.9173985	0.000192435	0.000685423	0.000998722	0.001430749	0.001844887	0.002016325	0.002402636	0.003076556	0.003429229	0.003757218	0.003886906
1.9230769	0.000173318	0.000712828	0.001021358	0.001418984	0.001858844	0.002013708	0.00243146	0.003120297	0.00349577	0.003845717	0.003982005
1.9288263	0.000168104	0.000760681	0.001055749	0.001410706	0.001871493	0.001992765	0.002439758	0.00311811	0.003506278	0.003866749	0.003993401
1.9345727	0.000173753	0.000823769	0.001100157	0.001411577	0.001886759	0.001963534	0.002435827	0.003086616	0.003477821	0.003839145	0.003941246
1.9403535	0.000185049	0.000890782	0.001148054	0.001417677	0.001903334	0.001932125	0.002424472	0.00303938	0.003424852	0.003781751	0.003846593
1.9462068	0.000194608	0.000950407	0.001192471	0.001422034	0.001917729	0.001898972	0.00240744	0.002986028	0.003357446	0.003707719	0.003727431
1.9520575	0.000200256	0.000993934	0.001228618	0.00141637	0.001926454	0.001861025	0.002383859	0.002927872	0.003278236	0.003620563	0.003589471
1.9579434	0.00020069	0.001020052	0.001252573	0.001394149	0.001923836	0.001811742	0.002348052	0.00285792	0.003183291	0.003514596	0.003427916
1.9639035	0.000194608	0.001028758	0.001259106	0.001350582	0.001902026	0.001742406	0.002292164	0.002764815	0.003066497	0.003380205	0.003235792
1.9698611	0.000178966	0.001020052	0.001242991	0.001283062	0.001854919	0.001646487	0.002209656	0.002642016	0.002922625	0.003213478	0.003007893
1.9758551	0.000150726	0.000993063	0.001201181	0.0011916	0.001779907	0.001522261	0.002099233	0.002487802	0.002751266	0.003016202	0.002746021
1.9818856	0.000110759	0.000947795	0.001136732	0.001080565	0.001679184	0.001374979	0.001964843	0.002308319	0.002555073	0.002795411	0.002457228
1.9879925	5.99368E-05	0.00088556	0.001055749	0.000955195	0.001556692	0.001209891	0.001812178	0.002113198	0.002340629	0.002559005	0.002148113
1.9940975	0	0.000810715	0.000965641	0.000821158	0.001420291	0.001034853	0.001647359	0.001910314	0.002116253	0.002315304	0.001827442
2.00024	-2.1715E-06	0.000728488	0.000870764	0.000682378	0.001276964	0.000854663	0.001475195	0.00170578	0.001888068	0.002068686	0.001501342
2.0064608	-7.3829E-06	0.000644972	0.000773733	0.000540599	0.001132378	0.000672809	0.001300921	0.001501342	0.00166131	0.001823517	0.001176794
2.0126799	-1.1726E-05	0.000563646	0.000677593	0.000397561	0.000990887	0.000493639	0.001129765	0.001301357	0.001440771	0.001583716	0.000859885
2.0189376	-1.1726E-05	0.000487552	0.000585389	0.000257613	0.000855969	0.000320193	0.000966511	0.001111042	0.001230796	0.001354939	0.000557123
2.0252754	-6.5144E-06	0.000416688	0.000499291	0.000124226	0.000728923	0.000155505	0.000815067	0.000934738	0.001033982	0.001140216	0.000271084
2.0316119	0	0.000350617	0.000418862	0	0.000608438	0	0.000674984	0.000772863	0.000850312	0.000940832	0
2.0379881	8.6859E-07	0.000288467	0.00034149	-1.0857E-05	0.000493204	-1.52E-05	0.000544947	0.000624095	0.000680638	0.000757636	-3.2571E-05
2.0444045	-1.3029E-06	0.000229368	0.000267173	-1.3463E-05	0.000384086	-2.128E-05	0.000424513	0.000486682	0.000527119	0.000590173	-4.9507E-05
2.0509034	-4.3429E-06	0.000173318	0.000198083	-9.1201E-06	0.000282383	-1.8674E-05	0.000313239	0.000358875	0.000388433	0.000436251	-4.9507E-05
2.0574015	-3.9086E-06	0.000118579	0.000134218	-1.3029E-06	0.000188525	-9.9887E-06	0.000209815	0.000238928	0.000260655	0.00029064	-3.5176E-05
2.0639409	-1.3029E-06	6.21086E-05	7.07958E-05	3.90867E-06	9.77273E-05	-1.3029E-06	0.000108153	0.000121619	0.000134218	0.00014812	-1.4766E-05
2.0705649	0	0	0	0	0	0	0	0	0	0	0
2.0771883	4.47346E-05	6.16742E-05	7.60082E-05	0.000100334	0.000115103	0.000104243	0.000121619	0.000119882	0.000119882	0.000127267	0.000149857

Table A.4: Absorbance data Fig 4.2 (2 of 2)

λ (μm)	Dry	Baseline	10%	20%	30%	40%	50%	60%	70%	80%	90%	100%
2.1530977	6.20272E-05	0.000204754	0.000461015	0.000416342	0.000453552	-0.00018851	0.002710496	0.002609597	0.002615535	0.002548716	0.002276726	0.002207825
2.1459682	2.70258E-05	7.90888E-05	0	0	0	-0.00034523	0.00114541	0.00109815	0.001096463	0.001065193	0.000938318	0.000903635
2.1388858	0	0	-0.00017112	-0.00016414	-0.0001793	-0.00034203	0	0	0	0	0	0
2.13185	0	0	0	0	0	0	0	0	0	0	0	0
2.1248603	-2.7957E-06	-0.00012625	-0.00046415	-0.00045023	-0.00049802	0.000833473	-0.00141583	-0.00141789	0.001503416	0.001558566	0.001596653	0.001645994
2.1179163	6.91159E-06	-0.00013624	-0.00053137	-0.0005216	-0.00057977	0.002060823	-0.00166221	-0.00167341	0.004186617	0.004287229	0.004287882	0.004379522
2.1110176	1.61273E-05	-8.1688E-05	-0.00035811	-0.00035987	-0.0004041	0.003537448	-0.00116166	-0.00118004	0.00763977	0.007783244	0.00769913	0.007832397
2.1041636	1.54024E-05	-2.1381E-05	-0.000132	-0.00014018	#VALUE!	0.005089376	-0.00045639	-0.00047242	0.011328807	0.011519781	0.011342756	0.011525045
2.097354	0	0	0	0	0	0.006580478	0	0	0.014802782	0.015051458	0.01480996	0.015054647
2.0905884	9.3191E-07	7.18395E-05	0.00118603	0.001231146	0.001394825	0.007944087	0.002946503	0.003022142	0.01781251	0.01813373	0.017878833	0.018201048
2.0838662	-3.7276E-06	9.10246E-05	0.002203636	0.002313731	0.002631942	0.009178004	0.005366933	0.005531497	0.020315489	0.020727805	0.020516211	0.020929043
2.0771872	-6.9374E-06	7.49204E-05	0.00309258	0.003285652	0.003750718	0.010318167	0.007363969	0.007630075	0.022408302	0.022930909	0.022811588	0.023326022
2.0705508	-5.8502E-06	4.02028E-05	0.00390438	0.004195216	0.004802835	0.01141081	0.009085742	0.00946578	0.024239636	0.02488908	0.024898373	0.0255247
2.0639567	0	0	0.004684545	0.005084714	0.005834103	0.012496777	0.010667635	0.011173957	0.02594922	0.026736763	0.026899742	0.027649035
2.0574044	-3.624E-06	0.000205739	0.005467819	0.005986771	0.00688116	0.013609344	0.012212151	0.012857441	0.027642387	0.028575254	0.02891021	0.029794016
2.0508937	-4.9183E-06	0.000422976	0.006280713	0.006927817	0.007974432	0.014777794	0.013793789	0.014592261	0.029393974	0.030479232	0.031001472	0.032031091
2.044424	-5.436E-06	0.000657872	0.007146023	0.007931195	0.009140674	0.016029429	0.015469694	0.016437693	0.03126088	0.032508303	0.033232189	0.034418375
2.037995	-4.3488E-06	0.000915982	0.008082967	0.009016044	0.010401624	0.017387001	0.017280345	0.018435391	0.033283861	0.034705993	0.035645042	0.036999784
2.0316063	0	0.001199321	0.009101074	0.010191185	0.011766956	0.018861496	0.019237175	0.02059633	0.035476951	0.037086809	0.038255145	0.039792052
2.0252575	1.55317E-06	0.001504585	0.010195663	0.011451578	0.013231722	0.020449483	0.021317879	0.022897453	0.037822553	0.039633097	0.041046844	0.04278006
2.0189483	2.84746E-06	0.001825167	0.011351365	0.012782789	0.01478082	0.022137919	0.023479064	0.025296214	0.040282474	0.04230667	0.043986147	0.045928383
2.0126783	2.40739E-06	0.002156469	0.012552115	0.014170697	0.01639925	0.023913814	0.025678848	0.027752501	0.042816711	0.045067959	0.047037751	0.04920127
2.0064471	9.06026E-07	0.00249646	0.013786601	0.015605287	0.018075922	0.025767122	0.027886381	0.030237218	0.04539252	0.047885529	0.050172835	0.052571198
2.0002543	0	0.002844403	0.015047974	0.017080736	0.019803063	0.027690722	0.030080695	0.032729897	0.047985258	0.050735871	0.053367945	0.056017659
1.9940997	-1.0976E-05	0.003199927	0.016330357	0.018591069	0.021572899	0.029676287	0.032244217	0.035212795	0.050573151	0.053597224	0.056598974	0.059518111
1.9879828	-1.7343E-05	0.003562633	0.017625164	0.020127441	0.023375245	0.031710902	0.034355137	0.037661042	0.053127729	0.056438965	0.059831552	0.06303665
1.9819034	-1.7343E-05	0.003930918	0.018918409	0.021674111	0.025193387	0.033773952	0.036376262	0.040032155	0.05560494	0.059211482	0.063012737	0.066515709
1.975861	-1.139E-05	0.004298706	0.020188994	0.023206156	0.027001431	0.035833747	0.038250791	0.042262843	0.057939853	0.061843262	0.066067277	0.069873855
1.9698553	0	0.004657804	0.021411417	0.024691561	0.02876448	0.037848931	0.039910796	0.044278196	0.060052469	0.064249564	0.068904122	0.073012794
1.9638861	-1.8275E-05	0.005001016	0.022561812	0.026099368	0.030445634	0.039774037	0.04129308	0.04600841	0.06186338	0.066347602	0.071429549	0.075831003
1.9579529	-3.0751E-05	0.005325395	0.023625955	0.027408676	0.032017687	0.041571102	0.042360119	0.047408335	0.063317002	0.068077384	0.073567462	0.078244409
1.9520554	-3.5928E-05	0.005633811	0.024604628	0.028614901	0.033469726	0.043216362	0.043114464	0.048469077	0.064395333	0.069411891	0.075270822	0.080197153
1.9461934	-2.8215E-05	0.005933234	0.025503836	0.029716478	0.034795112	0.044687889	0.043573911	0.049191355	0.065088796	0.070326297	0.076489944	0.081627617
1.9403665	0	0.006224724	0.026304294	0.030682485	0.035955801	0.045929822	0.043694495	0.04950854	0.06531767	0.070721448	0.077095937	0.082392387
1.9345743	0.000118807	0.00648895	0.026929927	0.03142142	0.03684675	0.046817963	0.043303098	0.049222637	0.064868339	0.070363005	0.076825768	0.082212861
1.9288167	0.000250545	0.006685457	0.027248924	0.031783366	0.037295887	0.047161033	0.042144054	0.048053896	0.063443674	0.068935309	0.075343665	0.08073698
1.9230932	0.000378488	0.006762723	0.027107636	0.031593822	0.03709882	0.046733521	0.040040983	0.045805509	0.060827845	0.066205488	0.072406076	0.077701787
1.9174035	0.000479517	0.006668345	0.026363428	0.030686069	0.036052489	0.045307636	0.037051963	0.042516193	0.057041804	0.062174875	0.068005599	0.073073834
1.9117475	0.000529458	0.006355805	0.024905939	0.028925427	0.033983624	0.042684432	0.033489075	0.038479918	0.052363806	0.05709875	0.062381417	0.067064945
1.9061247	0.00051554	0.00580367	0.022702829	0.026268488	0.030826359	0.038786005	0.029777964	0.034116274	0.047200566	0.051369763	0.055911594	0.060038974
1.9005349	0.00044925	0.00504776	0.019881994	0.022865883	0.026757025	0.033814831	0.026231144	0.029764768	0.041899046	0.045354759	0.048977747	0.052401042
1.8949778	0.000358954	0.004185022	0.016755074	0.019090489	0.022234194	0.028302939	0.022889185	0.025537905	0.03662282	0.039283197	0.041874843	0.044514168
1.8894531	0.000266241	0.003329708	0.013700408	0.015396925	0.017822974	0.022909105	0.019592082	0.021371906	0.031396904	0.033267288	0.034813258	0.036677883
1.8839605	0.00017852	0.002567307	0.011009286	0.012135453	0.013954681	0.01814126	0.016246425	0.017257019	0.026296181	0.027454311	0.028034025	0.02920763
1.8784997	0.000101951	0.001947438	0.008830103	0.00948393	0.010836476	0.014251901	0.013050103	0.013441104	0.021614714	0.022178862	0.021939087	0.022548424
1.8730705	4.86166E-05	0.001494117	0.007199288	0.007485809	0.00850043	0.011293018	0.010438293	0.010375482	0.017810811	0.017914575	0.017038601	0.017224374
1.8676726	2.57573E-05	0.001203889	0.006076566	0.006094154	0.006873822	0.009190166	0.008739024	0.008376669	0.01519255	0.014965764	0.013640729	0.013533868
1.8623057	2.47218E-05	0.001042954	0.005367903	0.005201226	0.005825314	0.007791151	0.007864633	0.007327084	0.013633678	0.013187104	0.011569971	0.011275324
1.8569696	2.89156E-05	0.000964805	0.004959278	0.004675178	0.005206649	0.006913667	0.007409783	0.006785966	0.012680483	0.012097416	0.010297067	0.009888018
1.851664	2.9278E-05	0.000933778	0.004750307	0.004397618	0.004882908	0.006390979	0.007043036	0.006390848	0.011945937	0.011283507	0.009365417	0.008889969
1.8463886	2.80354E-05	0.00093134	0.004666046	0.004276693	0.004743189	0.006090164	0.006745029	0.006096595	0.011356999	0.01065246	0.008657049	0.00814674
1.8411432	2.98217E-05	0.000946516	0.004650425	0.00424237	0.004697786	0.005910273	0.006704385	0.006070292	0.011061753	0.010338924	0.008298297	0.007773045
1.8359275	3.42744E-05	0.00096823	0.004660813	0.004243285	0.004683001	0.005782264	0.00705848	0.006433118	0.011177888	0.01045012	0.008394799	0.007865345
1.8307412	3.62936E-05	0.00098678	0.004671384	0.004250656	0.004667145	0.005670369	0.007762082	0.00713226	0.011656646	0.010929642	0.00888664	0.008357141
1.8255842	3.10125E-05	0.000997599	0.00467489	0.004256068	0.004645402	0.005564716	0.008657049	0.008010318	0.012342149	0.011616683	0.009606419	0.009077627
1.8204562	1.94926E-05	0.001002996	0.004678736	0.004264564	0.004628003	0.005470519	0.009598294	0.008926115	0.013087798	0.012362683	0.010397223	0.009869295
1.8153569	7.09283E-06	0.001008393	0.004693311	0.004283621	0.004625883	0.005395107	0.010495651	0.009794334	0.013798145	0.013072912	0.011156959	0.010630893
1.810286	0	0.001016825	0.00471995	0.004313451	0.004640404	0.005338839	0.011286403	0.010558055	0.014405417	0.013682856	0.01181627	0.011295037
1.8052434	0	0.001025595	0.004746094	0.004343727	0.00466042	0.005290518	0.011911348	0.011165777	0.014849495	0.014135155	0.01231677	0.011805656
1.8002289	-5.0218E-06	0.001031174	0.004754992	0.004360984	0.004670389	0.005234996	0.012328674	0.011582173	0.015088093	0.014389629	0.012619745	0.012125258
1.7952421	-7.0409E-06	0.001033691	0.00473594	0.0043568	0.004660682	0.005161538	0.012533331	0.011805896	0.015114895	0.014439964	0.012720358	0.012248494
1.7902829	-6.3161E-06	0.00103408	0.004684048	0.004325791	0.004624706	0.005062478	0.012549184	0.011859789	0.01495234	0.014307008	0.012639866	0.012194659
1.785351	-3.8311E-06	0.001029669	0.00459407	0.00426025	0.004553705	0.004928671	0.012402342	0.011765413	0.014626984	0.01401451	0.012402103	0.011985664
1.7804461	0	0.001015684	0.004458498	0.004149896	0.004435954	0.004749758	0.012104522	0.011526613	0.014149917	0.01357075	0.01201821	0.011630908
1.7755682	-3.1063E-06	0.000988986	0.004270864	0.003986377	0.004262211	0.004518078	0.011652285	0.011131808	0.013514427	0.01296747	0.011484881	0.011126124
1.7707169	-1.3979E-06	0.000947787	0.004024181	0.003762677	0.004024626	0.004227078	0.011022322	0.010552273	0.012695036	0.01218007	0.010784832	0.010453302
1.7658921	3.41696E-06	0.000885841	0.003700589	0.003462841	0.003705785	0.003862224	0.010156258	0.009731192	0.011636757	0.011157862	0.009875863	0.009571063
1.7610935	5.74671E-06	0.000791382	0.003268308	0.003058559	0.003275063	0.003397535	0.008966756	0.008589742	0.010260807	0.009829258	0.008694231	0.008419898
1.7563209	0	0.000653439	0.002700598	0.002525334	0.002706589	0.002812095	0.00739538	0.007079108	0.008516849	0.008149457	0.007199657	0.006964458
1.751574	-1.1027E-05	0.000474931	0.002011981	0.001876016	0.002015284	0.002120492	0.005502003	0.005263319	0.006465329	0.006178325	0.005446665	0.005260725
1.7468528	-2.6144E-05	0.00028186	0.001284703	0.001187095	0.001283691	0.001397214	0.003519598	0.003367298	0.004328327	0.004128597	0.003627181	0.003495668
1.742157	-3.3185E-05	0.000118962	0.000651832	0.000585106	0.000645688	0.000762026	0.001798029	0.00172346	0.002437702	0.002317453	0.002024906	0.001944552
1.7374863	-2.3349E-05	2.35827E-05	0.000226276	0.000180799	0.000216564	0.000317245	0.000630548	0.000608565	0.001074197	0.001013867	0.000877981	0.000837493
1.7328406	0	0	3.1582E-05	0	2.30391E-05	8.40858E-05	8.59499E-05	8.6183E-05	0.000310898	0.000288647	0.000245883	0.000231171
1.7282197	1.91819E-05	-1.9155E-06	0	-6.4555E-05	0	0	0	0	0	0	0	0
1.7236234	2.97181E-05	6.78217E-06	-1.6153E-05	-6.4969E-05	-2.4436E-05	-1.7291E-05	-0.00012677	-0.00011885	-0.000141	-0.00013743	-0.0001217	-0.00011777
1.7190515	2.86049E-05	5.77259E-06	-3.3547E-05	-6.5797E-05	-4.3434E-05	-3.5255E-05	-0.00020709	-0.00019446	-0.00022267	-0.00021656	-0.00019219	-0.00018598
1.7145037	1.66191E-05	-4.4524E-06	-5.2442E-05	-6.7557E-05	-5.9016E-05	-5.1717E-05	-0.0002282	-0.00021542	-0.0002355	-0.0002281	-0.00020233	-0.00019596
1.7099799	0	0	0	0	0	0	0	0	0	0	0	0
1.70548	-1.2322E-05	-0.00011057	-0.00037803	-0.00036091	-0.00038036	-0.00033737	-0.00091958	-0.00087794	-0.00090011	-0.0008504	-0.000758	-0.00073821
1.7010037	-9.5259E-06	-0.00014313	-0.00050386	-0.00048152	-0.00050826	-0.00044858	-0.00119728	-0.00114266	-0.00118215	-0.00111312	-0.00099423	-0.00096856
1.6965508	2.14855E-06	-0.00011124	-0.00041263	-0.00039546	-0.00041806	-0.00036722	-0.00095647	-0.00091261	-0.00095833	-0.00089938	-0.00080581	-0.00078426
1.6921211	7.89528E-06	-5.3995E-05	-0.00021444	-0.00020662	-0.00021873	-0.00019126	-0.00048525	-0.00046327	-0.00049595	-0.00046446	-0.00041791	-0.00040586
1.6877146	0	0	0	0	0	0	0	0	0	0	0	0
1.6833309	-5.6431E-06	-4.3486E-05	-0.00012791	-0.00012222	-0.00012594	-0.00011036	-0.00025532	-0.00025056	-0.00024476	-0.00024083	-0.00022008	-0.00021998
1.6789699	-1.258E-05	-6.9317E-05	-0.00020207	-0.00019286	-0.00019762	-0.00017361	-0.00037001	-0.0003621	-0.00034984	-0.00034296	-0.00031243	-0.00031642

Table A.5: Absorbance data Fig 4.5 (1 of 3)

λ (μm)	Dry	Baseline	10%	20%	30%	40%	50%	60%	70%	80%	90%	100%
1.6746315	-1.3719E-05	-6.2484E-05	-0.00018085	-0.00017314	-0.00017573	-0.00015493	-0.00027161	-0.00026644	-0.00025278	-0.00024802	-0.00022624	-0.00023581
1.6703155	-7.7657E-06	-3.013E-05	-8.5674E-05	-8.2775E-05	-8.2517E-05	-7.3251E-05	-7.0301E-05	-7.1025E-05	-6.1967E-05	-6.2536E-05	-5.8084E-05	-6.8282E-05
1.6660216	0	0	0	0	0	0	0	0	0	0	0	0
1.6617497	7.01517E-06	9.22156E-05	0.000323462	0.000304137	0.000320742	0.000277793	0.000814385	0.000772062	0.000785754	0.000751031	0.000664665	0.000649576
1.6574997	7.45521E-06	0.000135353	0.000481694	0.000452878	0.000477781	0.000413414	0.001209496	0.001147019	0.001169367	0.001120002	0.000988415	0.000968567
1.6532714	4.6336E-06	0.000128776	0.00046314	0.000435543	0.000459719	0.000397609	0.001186731	0.001126386	0.001149718	0.001104119	0.000971395	0.000952975
1.6490646	1.88966E-06	8.03316E-05	0.000290331	0.000273312	0.000288569	0.000249664	0.000772425	0.000733892	0.000749605	0.000721497	0.000633088	0.000620749
1.6448792	0	0	0	0	0	0	0	0	0	0	0	0
1.6407149	-6.1608E-06	1.16488E-05	5.9257E-05	5.78072E-05	6.0422E-05	5.22669E-05	0.000195587	0.000176423	0.000195923	0.000177821	0.000155758	0.000144442
1.6365717	-9.3706E-06	1.28396E-05	7.20466E-05	6.95871E-05	7.31599E-05	6.23379E-05	0.000199109	0.000173289	0.000200222	0.000175361	0.000153635	0.000140661
1.6324494	-8.7494E-06	1.02251E-05	6.00596E-05	5.67458E-05	6.04479E-05	5.0144E-05	0.000121189	9.89992E-05	0.000121319	0.000100138	8.71927E-05	7.87522E-05
1.6283477	-5.2289E-06	5.90206E-06	3.43003E-05	3.13231E-05	3.40414E-05	2.6974E-05	4.22997E-05	3.03135E-05	4.14972E-05	3.03394E-05	2.56538E-05	2.28061E-05
1.6242667	0	0	0	0	0	0	0	0	0	0	0	0
1.620206	-1.0354E-07	5.12544E-06	7.71409E-06	3.3393E-06	3.85703E-06	-1.553E-07	-3.7429E-05	-3.013E-05	-3.246E-05	-3.246E-05	-2.9457E-05	-3.246E-05
1.6161656	1.13898E-06	8.62009E-06	1.22184E-05	6.70452E-06	6.65275E-06	1.94143E-06	-4.3072E-05	-3.2926E-05	-3.5566E-05	-3.7585E-05	-3.4375E-05	-3.9863E-05
1.6121453	1.70847E-06	8.62009E-06	1.23219E-05	8.41302E-06	7.66233E-06	3.64996E-06	-3.1839E-05	-2.2831E-05	-2.5264E-05	-2.8784E-05	-2.7438E-05	-3.246E-05
1.6081449	9.3191E-07	4.99602E-06	7.71409E-06	6.60098E-06	5.61729E-06	2.74392E-06	-1.5531E-05	-1.0095E-05	-1.2063E-05	-1.4651E-05	-1.5376E-05	-1.7706E-05
1.6041644	0	0	0	0	0	0	0	0	0	0	0	0
1.6002035	-1.5014E-06	-2.7957E-06	2.69216E-06	2.53685E-06	3.31342E-06	-1.9673E-06	9.55202E-06	1.00439E-05	7.40344E-06	5.85025E-06	-1.2943E-06	-4.5041E-06
1.5962621	-3.1581E-06	-5.0218E-06	3.00277E-06	5.43607E-07	1.57905E-06	-3.9864E-06	1.42116E-05	1.15453E-05	9.75914E-06	6.91159E-06	-1.8638E-06	-8.8011E-06
1.59234	-4.2971E-06	-6.0055E-06	1.83789E-06	-2.7439E-06	-2.3815E-06	-5.1254E-06	1.39528E-05	6.85982E-06	7.01517E-06	3.98645E-06	-3.0027E-06	-1.1131E-05
1.5884372	-3.0545E-06	-4.0382E-06	8.02447E-07	-3.2099E-06	-3.6758E-06	-3.9346E-06	9.55202E-06	1.57905E-06	2.20032E-06	5.17723E-07	-3.3652E-06	-8.594E-06
1.5845535	0	0	0	0	0	0	0	0	0	0	0	0
1.5806888	9.57794E-07	-5.1772E-07	-7.1962E-06	-7.7657E-06	-1.0251E-05	-1.3616E-05	-1.17E-05	-1.491E-05	-1.4237E-05	-1.7602E-05	-2.1795E-05	-2.2365E-05
1.5768428	1.1131E-06	-1.3461E-06	-1.3202E-05	-1.2684E-05	-1.5428E-05	-2.1588E-05	-2.2883E-05	-2.3607E-05	-2.221E-05	-2.8732E-05	-3.4065E-05	-3.6187E-05
1.5730155	1.06133E-06	-1.7085E-06	-1.5117E-05	-1.3357E-05	-1.5117E-05	-2.2002E-05	-2.6765E-05	-2.5057E-05	-2.3866E-05	-3.1476E-05	-3.5411E-05	-3.8672E-05
1.5692068	7.50679E-07	-1.1907E-06	-1.0924E-05	-9.4742E-06	-9.9401E-06	-1.4962E-05	-1.9466E-05	-1.7809E-05	-1.7654E-05	-2.2779E-05	-2.4539E-05	-2.7335E-05
1.5654164	0	0	0	0	0	0	0	0	0	0	0	0
1.5616443	1.03545E-06	-1.7602E-06	-8.9047E-06	-1.6101E-05	-1.6515E-05	-1.8327E-05	-2.2624E-05	-2.1433E-05	-3.246E-05	-3.3547E-05	0.000419685	0.000445804
1.5578904	2.6145E-06	-2.4333E-06	-1.2063E-05	-2.3349E-05	-2.5368E-05	-2.6041E-05	-3.3081E-05	-3.1269E-05	-4.799E-05	-5.0268E-05	0.00085749	0.000910665
1.5541544	2.92511E-06	-2.8474E-06	-1.17E-05	-2.2676E-05	-2.6092E-05	-2.5057E-05	-3.2563E-05	-3.1528E-05	-4.7058E-05	-5.0009E-05	0.001315211	0.001395163
1.5504364	1.5014E-06	-2.6404E-06	-8.2834E-06	-1.4858E-05	-1.7913E-05	-1.6618E-05	-2.1588E-05	-2.1899E-05	-3.0648E-05	-3.2874E-05	0.001794156	0.001899207
1.546736	0	0	0	0	0	0	0	0	0	0	0.002293849	0.002422708
1.5430533	0	-9.3191E-07	-8.2317E-06	-9.9919E-06	-1.0095E-05	-1.5169E-05	-1.9518E-05	-1.8845E-05	0.00048794	0.000519557	0.002812329	0.002964955
1.5393881	5.43607E-07	-1.2943E-06	-1.227E-05	-1.5997E-05	-1.4755E-05	-2.2624E-05	-3.0182E-05	-2.6972E-05	0.000987636	0.001051076	0.003346507	0.003524921
1.5357403	5.43607E-07	-1.9155E-06	-1.2736E-05	-1.7654E-05	-1.5117E-05	-2.309E-05	-3.0907E-05	-2.6092E-05	0.00149874	0.001594496	0.003894977	0.004102099
1.5321097	3.88303E-07	-1.5532E-06	-8.4905E-06	-1.2425E-05	-1.0095E-05	-1.548E-05	-2.0294E-05	-1.6463E-05	0.002021083	0.002150694	0.004458105	0.004695902
1.5284962	0	0	0	0	0	0	0	0	0.002554027	0.002719222	0.005035583	0.005305532
1.5248998	-7.7656E-07	-1.0354E-06	-4.9701E-06	-7.4551E-06	-1.3305E-05	0.000327192	0.000502686	0.000531065	0.003096777	0.003298563	0.005626914	0.005930531
1.5213202	-1.812E-06	-2.7957E-06	-9.2671E-06	-1.2011E-05	-2.2676E-05	0.000660905	0.001007537	0.001063532	0.003648899	0.003887402	0.006231788	0.006571095
1.5177574	-2.2262E-06	-4.1417E-06	-1.1183E-05	-1.315E-05	-2.5057E-05	0.001004319	0.001513962	0.001599459	0.004209644	0.004485698	0.006851206	0.007227713
1.5142112	-1.6567E-06	-3.624E-06	-8.6976E-06	-9.4224E-06	-1.7602E-05	0.001359768	0.00202306	0.00214354	0.004779488	0.005095609	0.007487231	0.00790188
1.5106816	0	0	0	0	0	0.001726605	0.002536165	0.00269992	0.005359464	0.005720017	0.008140937	0.00859497
1.5071684	-1.0872E-06	-3.2099E-06	-7.3515E-06	0.000309629	0.000352658	0.002102804	0.003053475	0.003269247	0.005949085	0.00635817	0.008810158	0.009305617
1.5036715	1.08721E-06	-1.7085E-06	-8.0763E-06	0.000626296	0.000712344	0.002486749	0.003572994	0.003846607	0.006545052	0.007006205	0.009489089	0.010028607
1.5001907	3.70172E-06	1.06133E-06	-5.5913E-06	0.000948358	0.001076144	0.002876818	0.004090288	0.004422748	0.007142286	0.007658001	0.010171707	0.010757155
1.4967261	3.41696E-06	1.42375E-06	-2.8992E-06	0.001273747	0.001442585	0.003272716	0.004600925	0.004991249	0.007736442	0.00830872	0.010854019	0.01148613
1.4932774	0	0	0	0.001602083	0.001812767	0.003675814	0.005102419	0.005551318	0.008324208	0.008953623	0.011531983	0.012212417
1.4898446	-3.6242E-07	-5.1772E-07	0.000302609	0.001932643	0.002186829	0.004085218	0.005590701	0.00610308	0.0089003	0.00958702	0.012199025	0.012931946
1.4864275	-1.0872E-06	5.17723E-07	0.000606103	0.002262805	0.002561501	0.00449595	0.006060369	0.00664382	0.009458267	0.010202925	0.012847576	0.013639661
1.4830261	-2.278E-06	1.63082E-06	0.0009075	0.002587905	0.0029311	0.004900972	0.006506529	0.007168602	0.009991469	0.010795315	0.013470501	0.014327876
1.4796402	-2.5368E-06	1.88966E-06	0.001203033	0.002903607	0.003291651	0.005294448	0.006927423	0.007672492	0.010495094	0.01135931	0.014062368	0.01498752
1.4762697	0	0	0.001486974	0.003203996	0.003637361	0.005669792	0.00732274	0.0081522	0.010967312	0.011890969	0.014619863	0.015609983
1.4729145	-2.0707E-07	1.51694E-05	0.001751763	0.00348142	0.003957929	0.00601622	0.0076961	0.00860804	0.011410703	0.012391448	0.015143441	0.016192146
1.4695746	4.65955E-07	2.24178E-05	0.001991774	0.003729439	0.004242867	0.006321817	0.008054802	0.009044324	0.011829889	0.012863387	0.015633811	0.016733282
1.4662498	1.39787E-06	2.2159E-05	0.002204937	0.003944893	0.004486325	0.006578349	0.00840013	0.009460674	0.012221283	0.013301487	0.016081781	0.017225559
1.4629399	1.52729E-06	1.49882E-05	0.002390197	0.004125461	0.004687319	0.006781996	0.008716125	0.00984157	0.012566131	0.013685394	0.016462132	0.017645949
1.459645	0	0	0.002545669	0.004268981	0.004847359	0.006933551	0.008975424	0.010159544	0.012836164	0.01398668	0.016743209	0.017963108
1.4563649	-3.0545E-06	6.00855E-05	0.002670514	0.004376515	0.004969777	0.007038327	0.009157567	0.010392318	0.013009532	0.014186209	0.016906436	0.018155835
1.4530995	-4.2971E-06	0.000114069	0.002767779	0.004453162	0.005059493	0.007104525	0.009262908	0.01053681	0.013084676	0.014285018	0.016958167	0.018227449
1.4498488	-3.4169E-06	0.000163371	0.002841172	0.004504294	0.005120387	0.007138154	0.009308579	0.010608717	0.013080755	0.014302407	0.01692428	0.018202748
1.4466125	-1.5014E-06	0.000208432	0.002894668	0.004533354	0.005154911	0.007141733	0.009315878	0.010629832	0.013024869	0.01426129	0.016832242	0.018111599
1.4433906	0	0.000250079	0.002931778	0.004542431	0.005165206	0.007116392	0.009297233	0.010614393	0.012932933	0.014173826	0.01669379	0.017969691
1.4401831	-1.1907E-06	0.000289631	0.002954921	0.004533119	0.005152737	0.007063163	0.009252119	0.010563386	0.012804704	0.014038759	0.016503512	0.017773351
1.4369898	-2.485E-06	0.000325845	0.00296188	0.004503509	0.005115358	0.006979767	0.009172055	0.010469106	0.012631205	0.013849373	0.016251021	0.017511173
1.4338106	-3.6758E-06	0.000356726	0.002949292	0.004449632	0.005049881	0.006862724	0.009050218	0.010325272	0.012405272	0.013601759	0.01593127	0.017175305
1.4306455	-3.2616E-06	0.000382401	0.002916793	0.004369926	0.004955062	0.006711483	0.008879903	0.010125707	0.012119029	0.013289716	0.015539873	0.016760024
1.4274943	0	0.000403335	0.00286504	0.004264302	0.004831182	0.006526552	0.008647384	0.009857141	0.011755998	0.012896879	0.015061909	0.016251988
1.4243569	1.24252E-06	0.000418597	0.002791487	0.004131367	0.00467646	0.006306031	0.008330277	0.009498667	0.011294294	0.012400185	0.014473952	0.015629706
1.4212333	1.76024E-06	0.000425308	0.002689528	0.003966706	0.004486352	0.006044121	0.007906414	0.009028518	0.010713587	0.011777382	0.013751652	0.01486913
1.4181234	1.86378E-06	0.00042212	0.002552804	0.003764818	0.00425646	0.005734129	0.00735765	0.008427209	0.009996078	0.011009419	0.012874133	0.01394709
1.4150271	1.60494E-06	0.000406833	0.002375283	0.003519128	0.003980525	0.005368767	0.006671972	0.007679316	0.009127271	0.010081963	0.011826431	0.012846029
1.4119442	0	0.000378022	0.00215496	0.003225354	0.003653233	0.004943149	0.005857585	0.006789569	0.008110316	0.008999737	0.010612616	0.011568322
1.4088748	4.2971E-06	0.000337114	0.001897673	0.002886356	0.003275558	0.004459282	0.004953753	0.005796561	0.006980977	0.00779795	0.009266583	0.01014815
1.4058186	8.1024E-06	0.000288336	0.001616477	0.002512862	0.002858448	0.003928619	0.004023737	0.004766978	0.005805244	0.006540112	0.00784924	0.00864844
1.4027758	9.57791E-06	0.000234409	0.001325155	0.002117188	0.002416279	0.003365159	0.003142118	0.003781008	0.004667877	0.005309017	0.006442471	0.007154996
1.399746	5.95383E-06	0.0001772	0.001035819	0.001712155	0.001963534	0.002784452	0.002387985	0.002922969	0.00365801	0.004195451	0.005141552	0.005766498
1.3967293	0	0.000123908	0.000764956	0.001318534	0.001521703	0.002212769	0.001810974	0.00224472	0.002827676	0.003256363	0.004014436	0.004551979
1.3937256	7.66233E-06	8.28948E-05	0.00053262	0.000964598	0.001122753	0.001688688	0.001367402	0.00170254	0.002134513	0.002455951	0.003035749	0.003486326
1.3907348	1.48329E-05	5.3173E-05	0.000349912	0.000670887	0.000793664	0.001243191	0.000931184	0.001170509	0.001463649	0.001684816	0.00209924	0.002466937
1.3877567	1.32279E-05	2.68963E-05	0.000211643	0.000437253	0.000537829	0.0008792	0.000444016	0.000592779	0.000771647	0.000904232	0.001164331	0.001460792
1.3847914	3.75349E-06	4.6336E-06	0.000106922	0.000250312	0.000336389	0.000576812	5.20339E-05	0.00011992	0.000206334	0.000265127	0.000384033	0.000626841
1.3818388	0	0	3.31612E-05	0.000101925	0.000171891	0.000320017	0	0	0	0	0	0.000205765
1.3788987	-6.4197E-06	-3.686E-05	0	0	5.01699E-05	0.000118211	0.000139341	0.000122328	9.72386E-05	8.07976E-05	7.60596E-05	0.000236351
1.3759711	-1.8638E-06	-4.8766E-05	-9.3594E-05	-0.00011362	0	0	0.000409994	0.000387686	0.000345456	0.000322685	0.000329239	0.000450339
1.3730559	2.97688E-06	-4.4263E-05	-0.00011999	-0.00014473	-8.2361E-05	-8.4898E-05	0.000488665	0.000469903	0.000428935	0.000408155	0.000425256	0.000511808

Table A.6: Absorbance data Fig 4.5 (2 of 3)

λ (μm)	Dry	Baseline	10%	20%	30%	40%	50%	60%	70%	80%	90%	100%
1.3701531	3.88291E-06	-2.6869E-05	-8.0912E-05	-9.6233E-05	-6.8023E-05	-7.0249E-05	0.000287119	0.000276939	0.000253394	0.000240988	0.000259766	0.000315613
1.3672624	0	0	0	0	0	0	0	0	0	0	1.7784E-05	4.54323E-05
1.364384	2.04763E-05	2.02174E-05	5.14902E-05	6.39431E-05	9.66948E-05	9.05845E-05	-0.00073919	-0.00074519	-0.00073945	-0.00074121	0	0
1.3615176	3.02876E-05	2.94851E-05	7.62668E-05	9.23969E-05	0.000137994	0.000131624	-0.00106478	-0.0010749	-0.00106664	-0.0010702	-0.00053179	-0.00053272
1.3586633	3.01064E-05	2.54208E-05	6.72311E-05	7.96584E-05	0.000118211	0.000115467	-0.00095471	-0.00096458	-0.00095745	-0.0009622	-0.00060939	-0.00061058
1.3558209	2.36863E-05	1.34868E-05	3.61901E-05	4.19373E-05	6.19754E-05	6.21307E-05	-0.00053416	-0.0005398	-0.00053634	-0.00054011	-0.00036411	-0.00036479
1.3529904	1.44446E-05	0	0	0	0	0	0	0	0	0	0	0
1.3501717	5.74671E-06	-3.3652E-06	-1.6722E-05	-1.9725E-05	-3.4479E-05	-3.9552E-05	0.000434169	0.00043163	0.000422302	0.000425437	0.000432381	0.000431785
1.3473647	0	-3.9864E-06	-2.0864E-05	-2.4798E-05	-4.7317E-05	-5.5341E-05	0.000668294	0.000663213	0.000647347	0.00065388	0.000663239	0.000662098
1.3445693	-5.1772E-06	-3.5205E-06	-1.5583E-05	-1.9E-05	-4.1985E-05	-4.8663E-05	0.000656369	0.000650743	0.000633296	0.000641306	0.000649006	0.000647736
1.3417855	-5.902E-06	-2.8474E-06	-7.1962E-06	-9.06E-06	-2.4643E-05	-2.7542E-05	0.000415591	0.000412145	0.000400433	0.000406082	0.000409735	0.000409113
1.3390132	0	0	0	0	0	0	0	0	0	0	0	0
1.3362524	-3.1065E-07	3.98645E-06	2.26767E-05	1.79393E-05	1.81465E-05	1.05098E-05	8.1652E-05	8.15484E-05	9.54779E-05	8.09012E-05	7.71211E-05	7.76389E-05
1.3335029	2.27797E-06	8.54244E-06	3.50769E-05	2.75176E-05	2.88638E-05	1.50918E-05	0.000102106	9.98795E-05	0.000123105	0.000100035	9.56592E-05	9.48824E-05
1.3307647	3.00277E-06	9.62967E-06	3.3653E-05	2.64304E-05	2.72329E-05	1.24772E-05	8.91345E-05	8.39563E-05	0.000108113	8.59758E-05	8.26359E-05	7.98655E-05

Table A.7: Absorbance data Fig 4.5 (3 of 3)

λ (μm)	Ice T=0 C	Ice T=-5 C	Liquid Water T=10 C	Liquid Water T=25 C
1.36151673	-8.68502E-05	-4.34273E-05	-8.68502E-05	-4.34273E-05
1.362949313	-4.34273E-05	-4.34273E-05	-4.34273E-05	-4.34273E-05
1.364384915	0	0	0	0
1.365821678	0	0	-4.34273E-05	0
1.36726334	4.34316E-05	0	-4.34273E-05	-4.34273E-05
1.368706176	4.34316E-05	4.34316E-05	-4.34273E-05	-4.34273E-05
1.370153937	4.34316E-05	4.34316E-05	0	-4.34273E-05
1.371602883	4.34316E-05	4.34316E-05	0	-4.34273E-05
1.373056781	4.34316E-05	4.34316E-05	0	-4.34273E-05
1.374511876	4.34316E-05	0	0	0
1.375971952	0	0	0	0
1.377433236	-8.68502E-05	-4.34273E-05	0	0
1.378899528	-0.000130269	-8.68502E-05	0	0
1.38036704	-0.000173683	-0.000130269	4.34316E-05	4.34316E-05
1.381839588	-0.000173683	-0.000130269	0.000130308	0.000130308
1.383313368	-0.000173683	-0.000130269	0.000304113	0.000304113
1.384792212	-0.000130269	-0.000130269	0.000521466	0.000477987
1.3862723	-8.68502E-05	-4.34273E-05	0.000825944	0.000738929
1.387757481	0	0	0.001174181	0.00104356
1.389243918	0	-4.34273E-05	0.001522697	0.001391971
1.390735477	-4.34273E-05	-4.34273E-05	0.001958736	0.001740662
1.392228303	-4.34273E-05	-4.34273E-05	0.002395213	0.002133274
1.393726281	0	-4.34273E-05	0.002875844	0.002569926
1.395225538	0	-4.34273E-05	0.003400777	0.003007018
1.396729976	0	0	0.003926346	0.003488328
1.398235706	4.34316E-05	4.34316E-05	0.004452551	0.004014002
1.399746646	8.68676E-05	4.34316E-05	0.005023326	0.00449643
1.401258891	0.000130308	0.000130308	0.005594853	0.005023326
1.402776375	0.000217202	0.000173753	0.006167133	0.005550863
1.404295177	0.000304113	0.000260655	0.006740169	0.006079041
1.405819248	0.000434512	0.000347575	0.007313961	0.006607863
1.40734465	0.00056495	0.000477987	0.007844289	0.007093182
1.408875351	0.000695428	0.000608438	0.008375265	0.00762324
1.410407396	0.000825944	0.000738929	0.008906892	0.008109696
1.41194477	0.0009565	0.000869459	0.009394789	0.008596697
1.413483502	0.001087096	0.001000028	0.009838807	0.0090399
1.415027593	0.00121773	0.001130636	0.010238812	0.009483556
1.416573055	0.001348404	0.001261284	0.010639186	0.009883234
1.418123907	0.001479117	0.001391971	0.010995384	0.01028328
1.419676143	0.001566281	0.001522697	0.011351875	0.010639186
1.421233801	0.00169706	0.001653463	0.011619435	0.010995384
1.422792857	0.001827878	0.001784268	0.011931797	0.011307297
1.424357366	0.001958736	0.001915112	0.012199714	0.011619435
1.425923285	0.002089633	0.002045996	0.012423105	0.011931797
1.42749469	0.002220569	0.002220569	0.012646611	0.012244383
1.429067519	0.002395213	0.002395213	0.012825499	0.012512494
1.430645865	0.002526241	0.002526241	0.01300446	0.01278077
1.43222565	0.002701008	0.00274471	0.01313873	0.01300446
1.433810984	0.002875844	0.002919565	0.013273041	0.013273041
1.43539777	0.003050752	0.003138232	0.013407393	0.013496985
1.436990138	0.003269485	0.003357009	0.013541787	0.013676223
1.438583973	0.00344455	0.003575896	0.013631406	0.013855535
1.440183422	0.003663482	0.003794894	0.013676223	0.014034922
1.441784352	0.003882524	0.004057837	0.01376587	0.014214382
1.443390929	0.00414552	0.004320939	0.0138107	0.014349026
1.444999003	0.004364805	0.004584201	0.0138107	0.014483712
1.446612756	0.004628094	0.004891542	0.013855535	0.014573526
1.448228021	0.004935466	0.00515515	0.013855535	0.014663358
1.449848998	0.005199101	0.005462896	0.013855535	0.014753209
1.451471502	0.005506877	0.005814872	0.013855535	0.014798142
1.453099752	0.005814872	0.006123085	0.0138107	0.014843079
1.454729544	0.006167133	0.006475597	0.01376587	0.01488802
1.456365117	0.006475597	0.006828395	0.013676223	0.01488802
1.458002245	0.006828395	0.00718148	0.013541787	0.014843079
1.459645189	0.007137329	0.007534852	0.013452187	0.014798142
1.461289705	0.007490665	0.007888512	0.013273041	0.014753209
1.462940071	0.007844289	0.008286724	0.013093969	0.01461844
1.464592023	0.00824246	0.008685302	0.01291497	0.014528617
1.466249861	0.008596697	0.0090399	0.012691326	0.014349026
1.467909301	0.008951224	0.00943917	0.012467797	0.014214382
1.469574661	0.009306039	0.009794385	0.012244383	0.014034922
1.47124164	0.009661145	0.010194349	0.011976438	0.0138107
1.472914574	0.009972101	0.010505687	0.011708658	0.013586595
1.474589143	0.01028328	0.010861776	0.011396457	0.01331782
1.476269703	0.010550182	0.011173593	0.011084479	0.013049212
1.477954098	0.010817249	0.011441043	0.010772726	0.01278077
1.479640152	0.01103993	0.011708658	0.010461197	0.012512494
1.481332251	0.011262725	0.011931797	0.010105436	0.012199714
1.483026026	0.011396457	0.01211039	0.009749967	0.01188716
1.484725882	0.01153023	0.012244383	0.009394789	0.01153023
1.486427431	0.011619435	0.012378418	0.0090399	0.011218157
1.488135099	0.011664044	0.012467797	0.008685302	0.010861776
1.489844475	0.011664044	0.012512494	0.008330993	0.010505687
1.491560008	0.011664044	0.012512494	0.007976972	0.010194349
1.493277266	0.011619435	0.012512494	0.00762324	0.009838807
1.661750654	0.000304113	0.000260655	0.000130308	0.000130308
1.663882437	0.000347575	0.000304113	0.000130308	0.000173753
1.666022471	0.000347575	0.000304113	0.000130308	0.000173753
1.668165235	0.000260655	0.000217202	8.68676E-05	0.000130308
1.670316308	0.000173753	0.000173753	4.34316E-05	8.68676E-05
1.672470138	8.68676E-05	8.68676E-05	4.34316E-05	4.34316E-05
1.674632334	0	0	0	0
1.676797317	-0.00013027	-0.00013027	-4.34273E-05	-8.685E-05
1.678970724	-0.00021709	-0.00021709	-8.68502E-05	-0.00013027
1.681146946	-0.0003039	-0.0002605	-8.68502E-05	-0.00013027
1.68333165	-0.0003039	-0.0002605	-8.68502E-05	-0.00013027
1.685519199	-0.0002605	-0.0002605	-8.68502E-05	-0.00013027
1.687715289	-0.00021709	-0.00017368	-8.68502E-05	-8.685E-05
1.689914254	-0.00013027	-8.685E-05	-4.34273E-05	-4.3427E-05
1.692121819	0	0	0	0
1.694332289	-0.00021709	-0.00021709	-8.68502E-05	-0.00013027
1.69655142	-0.00039069	-0.00039069	-0.000173683	-0.00021709
1.698773486	-0.00052084	-0.00052084	-0.000260499	-0.0002605
1.701004273	-0.00060759	-0.00056422	-0.000260499	-0.0003039
1.703238026	-0.00056422	-0.00052084	-0.000260499	-0.0003039
1.705480562	-0.00047746	-0.00043408	-0.000217093	-0.0002605
1.707726094	-0.0002605	-0.0002605	-0.000130269	-0.00013027
1.709980472	0	0	0	0
1.712237878	-8.685E-05	-8.685E-05	-4.34273E-05	-4.3427E-05
1.714504191	-0.00017368	-0.00013027	-8.68502E-05	-8.685E-05
1.716773564	-0.00017368	-0.00013027	-8.68502E-05	-8.685E-05
1.719051908	-0.00017368	-0.00013027	-8.68502E-05	-8.685E-05
1.721333345	-0.00013027	-0.00013027	-8.68502E-05	-8.685E-05
1.723623816	-8.685E-05	-8.685E-05	-4.34273E-05	-8.685E-05
1.725917411	-4.3427E-05	-4.3427E-05	-4.34273E-05	-4.3427E-05
1.728220106	0	0	0	0
1.730525959	-4.3427E-05	-4.3427E-05	-4.34273E-05	-4.3427E-05
1.732840975	0	-4.3427E-05	-4.34273E-05	-4.3427E-05
1.735159184	0	0	-4.34273E-05	0
1.737486621	0.000130308	8.68676E-05	0	4.34316E-05
1.739817284	0.000304113	0.000217202	4.34316E-05	0.000130308
1.742157244	0.000608438	0.000477987	0.000130308	0.000304113
1.744500462	0.0009565	0.000782434	0.000260655	0.000477987
1.746853044	0.001391971	0.001174181	0.000391041	0.000695428
1.74920892	0.001871493	0.001566281	0.00056495	0.000912977
1.751574227	0.002351545	0.002002364	0.000738929	0.001174181
1.753942864	0.002832129	0.002395213	0.000912977	0.001391971
1.756320999	0.003269485	0.002788417	0.00104356	0.001653463
1.7587025	0.003707281	0.003138232	0.00121773	0.001871493
1.761093569	0.004057837	0.00344455	0.001304842	0.002045996
1.763488038	0.004364805	0.003751085	0.001391971	0.002220569
1.765892146	0.004671991	0.003970172	0.001435542	0.002351545
1.768299691	0.004891542	0.00414552	0.001479117	0.002438884
1.770716946	0.005067263	0.004277078	0.001522697	0.002526241
1.773140818	0.005199101	0.004408676	0.001522697	0.002613616
1.775568182	0.005287015	0.00449643	0.001479117	0.002613616
1.778005362	0.005374946	0.004540313	0.001435542	0.002657309
1.780446073	0.005462896	0.004584201	0.001391971	0.002657309
1.782896672	0.005462896	0.004584201	0.001348404	0.002613616
1.785350839	0.005462896	0.004584201	0.001261284	0.002613616
1.787814968	0.005462896	0.004540313	0.001174181	0.002526241
1.790282704	0.005418919	0.00449643	0.00104356	0.002482561
1.792760475	0.005330978	0.004408676	0.000912977	0.002351545
1.795241891	0.005243055	0.004320939	0.000782434	0.002264223
1.797733418	0.00515515	0.004189368	0.000608438	0.002133274
1.800228629	0.004979394	0.004057837	0.000434512	0.002002364
1.802734026	0.004803708	0.003926346	0.000217202	0.001827878
1.805243148	0.004628094	0.003707281	0	0.001653463
1.807762532	0.004408676	0.00353211	4.34316E-05	0.001479117
1.810285681	0.004189368	0.003313244	4.34316E-05	0.001261284
1.812819169	0.003926346	0.003094489	4.34316E-05	0.00104356
1.815356463	0.003663482	0.002832129	4.34316E-05	0.000825944
1.817904175	0.003400777	0.002569926	0	0.000608438
1.820455733	0.003138232	0.002351545	0	0.000391041
1.823017787	0.002875844	0.002089633	0	0.000217202
1.82558373	0.002613616	0.001827878	0	0
1.828160249	0.002307882	0.001566281	-8.68502E-05	-8.685E-05
1.830740699	0.002045996	0.001304842	-0.000173683	-0.00013027
1.833331806	0.001784268	0.001087096	-0.000217093	-0.00017368
1.835926886	0.001566281	0.000825944	-0.000260499	-0.00017368
1.838532704	0.001304842	0.000608438	-0.000217093	-0.00017368
1.841142539	0.001130636	0.000391041	-0.000130269	-0.00013027
1.843763194	0.000912977	0.000173753	0	0
1.846387911	0.000782434	0	8.68676E-05	4.34316E-05
1.849023531	0.000608438	-4.3427E-05	0.000260655	0.000173753
1.851663257	0.000477987	-4.3427E-05	0.000477987	0.000347575
1.854313969	0.000391041	-4.3427E-05	0.000825944	0.000651931
1.856968833	0.000260655	-4.3427E-05	0.001261284	0.00104356
1.859634768	0.000173753	-4.3427E-05	0.001871493	0.001566281
1.8623049	8.68676E-05	-4.3427E-05	0.002613616	0.002264223

Table A.8 Absorbance data Fig 4.8 (1 of 2)

λ (μm)	Ice T=0 C	Ice T=-5 C	Liquid Water T=10 C	Liquid Water T=25 C
1.495000718	0.01153023	0.012467797	0.007225636	0.009483556
1.496725912	0.011441043	0.012378418	0.006872515	0.009128595
1.498457338	0.011307297	0.012289057	0.006519681	0.008773924
1.500190524	0.011173593	0.012199714	0.006123085	0.008419543
1.50192998	0.01103993	0.012065735	0.005770859	0.00806545
1.503671213	0.010861776	0.011931797	0.005374946	0.007711646
1.505418755	0.010683695	0.011753277	0.005023326	0.00735813
1.507168091	0.010461197	0.01157483	0.004671991	0.007004902
1.508923775	0.01028328	0.011396457	0.004320939	0.00665196
1.510681272	0.010060987	0.011218157	0.003970172	0.006299305
1.512445155	0.009838807	0.01103993	0.003619687	0.005946936
1.514210869	0.009616741	0.010861776	0.003269485	0.005638848
1.515983009	0.009394789	0.010639186	0.002919565	0.005287015
1.517756998	0.009172949	0.010416711	0.002569926	0.004935466
1.519537453	0.008906892	0.010194349	0.002220569	0.004628094
1.521319775	0.008685302	0.010016542	0.001915112	0.004277078
1.523108604	0.008419543	0.009794385	0.001566281	0.003970172
1.524899319	0.008198201	0.009572342	0.001261284	0.003619687
1.52669658	0.00793274	0.009306039	0.0009565	0.003313244
1.528495746	0.007667441	0.009084245	0.000608438	0.002963289
1.5303015	0.007402304	0.008862565	0.000304113	0.002657309
1.532109178	0.007137329	0.008596697	0	0.002351545
1.533923485	0.006872515	0.008375265	0	0.002045996
1.535739735	0.006607863	0.008109696	-4.34273E-05	0.001740662
1.537562656	0.006299305	0.007844289	-4.34273E-05	0.001435542
1.539387539	0.006035002	0.007579044	-4.34273E-05	0.001130636
1.541219135	0.005726851	0.007313961	-4.34273E-05	0.000869459
1.543052714	0.005462896	0.007049039	-4.34273E-05	0.00056495
1.544893047	0.00515515	0.00678428	0	0.000260655
1.546735383	0.004847623	0.006519681	0	0
1.548584516	0.004540313	0.006255243	0	0
1.550435672	0.004233221	0.005946936	-4.34273E-05	0
1.552293669	0.003970172	0.005682847	-4.34273E-05	-4.34273E-05
1.554153709	0.003663482	0.005418919	-4.34273E-05	-4.34273E-05
1.556020633	0.003357009	0.005111205	-4.34273E-05	-4.34273E-05
1.55788962	0.003050752	0.004803708	-4.34273E-05	-4.34273E-05
1.559765536	0.002701008	0.004540313	0	0
1.561643536	0.002395213	0.004233221	0	0
1.563528509	0.002089633	0.003970172	0	0
1.565415587	0.001784268	0.003663482	0	-4.34273E-05
1.567309682	0.001479117	0.003400777	-4.34273E-05	-4.34273E-05
1.569205903	0.001174181	0.003094489	-4.34273E-05	-4.34273E-05
1.571109187	0.000869459	0.002832129	-4.34273E-05	-4.34273E-05
1.57301462	0.00056495	0.002569926	0	0
1.57492716	0.000304113	0.002307882	0	0
1.57684187	0	0.002002364	0	0
1.578763733	0	0.001740662	0	0
1.580687789	0	0.001479117	0	0
1.582619045	0	0.001261284	0	0
1.584552514	0	0.001000028	0	0
1.586493231	0	0.000738929	0	0
1.588436185	0	0.000477987	0	0
1.590386432	0	0.000260655	0	0
1.592338939	0	0	0	0
1.594298788	0	0	0	0
1.596260918	0	0	0	0
1.598230439	0	0	0	0
1.600202266	0	0	0	0
1.60218153	0	0	0	0
1.604163124	0	0	0	0
1.606152205	0	0	0	0
1.608143639	0	0	0	0
1.61014261	0	0	0	0
1.612146557	0	0	0	0
1.614152893	0	0	0	0
1.61616684	0	0	0	0
1.618183201	0	0	0	0
1.620207225	0	0	0	0
1.622233686	0	0	0	0
1.624267861	0	0	0	0
1.626304499	4.34316E-05	4.34316E-05	0	0
1.628348903	8.68676E-05	8.68676E-05	0	4.34316E-05
1.630395795	8.68676E-05	8.68676E-05	4.34316E-05	4.34316E-05
1.632450504	8.68676E-05	0.000130308	4.34316E-05	4.34316E-05
1.634507727	0.000130308	0.000130308	4.34316E-05	4.34316E-05
1.63657282	8.68676E-05	8.68676E-05	4.34316E-05	4.34316E-05
1.638640453	4.34316E-05	4.34316E-05	0	4.34316E-05
1.640716008	0	0	0	0
1.64279413	0.000173753	0.000173753	8.68676E-05	8.68676E-05
1.644880228	0.000347575	0.000304113	0.000130308	0.000173753
1.646968918	0.000434512	0.000434512	0.000173753	0.000217202
1.649065639	0.000477987	0.000477987	0.000173753	0.000260655
1.651164979	0.000477987	0.000477987	0.000173753	0.000217202
1.653272405	0.000391041	0.000391041	0.000173753	0.000173753
1.655382476	0.000217202	0.000217202	8.68676E-05	0.000130308
1.657500688	0	0	0	0
1.659621573	0.000173753	0.000173753	8.68676E-05	8.68676E-05
1.86498619	4.34316E-05	0	0.003619687	0.003138232
1.867671723	0	0	0.004847623	0.004277078
1.8703685	0	0	0.006343371	0.005638848
1.873069568	0	-4.3427E-05	0.008198201	0.007313961
1.875781967	4.34316E-05	-4.3427E-05	0.010372229	0.009306039
1.878498704	0.000130308	-8.685E-05	0.012870232	0.011619435
1.881226861	0.000260655	-8.685E-05	0.015697768	0.014259259
1.883959404	0.000391041	-8.685E-05	0.018861217	0.017186238
1.886703457	0.00056495	-8.685E-05	0.022276395	0.020406104
1.889451946	0.000825944	0	0.025902996	0.023879382
1.892212034	0.001174181	4.34316E-05	0.02974613	0.02751945
1.894976607	0.00160987	0.000173753	0.033670505	0.031376979
1.897752871	0.002220569	0.000434512	0.037630664	0.035269079
1.90053367	0.002919565	0.000912977	0.041579472	0.039148846
1.903326253	0.003794894	0.001566281	0.045371622	0.042967684
1.906123421	0.004803708	0.002395213	0.048954052	0.046626949
1.908932468	0.005946936	0.00344455	0.052272273	0.050024822
1.911746151	0.007225636	0.004628094	0.05527064	0.053203973
1.914571806	0.008596697	0.005990967	0.057892691	0.056011125
1.91740215	0.010016542	0.007446482	0.060131456	0.05843888
1.920244562	0.011441043	0.008951224	0.061980903	0.060530669
1.923091716	0.012870232	0.010505687	0.063435995	0.062281556
1.925951035	0.01430414	0.012021084	0.064492734	0.06363708
1.928815148	0.015697768	0.013541787	0.065198658	0.064643907
1.931691524	0.017050711	0.015022874	0.065602559	0.065299598
1.93457275	0.018362575	0.016509028	0.065653073	0.065653073
1.937466337	0.019678414	0.017909761	0.065451052	0.065754119
1.940364827	0.020907099	0.019315026	0.064996849	0.065602559
1.94327578	0.022139271	0.020633758	0.064341614	0.065198658
1.946191692	0.023374948	0.021910827	0.063536526	0.06459351
1.949120167	0.024522237	0.023145853	0.06253226	0.063838259
1.952053658	0.025580426	0.024338467	0.061430244	0.062933688
1.954999814	0.026595026	0.025442255	0.060181337	0.061880731
1.957951043	0.02751945	0.026410377	0.05883654	0.060730414
1.960915041	0.028353118	0.027288159	0.05744632	0.059433714
1.96388417	0.029049066	0.028075051	0.055912321	0.058041583
1.966866172	0.029653124	0.028724151	0.054334501	0.056554951
1.969857244	0.030118356	0.02923484	0.052713355	0.054974799
1.972853535	0.030444316	0.029606628	0.051000546	0.053351266
1.975862859	0.030677294	0.029839157	0.049294465	0.051684859
1.978877462	0.030723905	0.029978734	0.047498152	0.049976093
1.981905205	0.030723905	0.029978734	0.045709238	0.048225492
1.984938288	0.030584088	0.029885678	0.043927663	0.046433586
1.987984621	0.030304589	0.029653124	0.042105513	0.044649043
1.991036354	0.029978734	0.029327757	0.040290976	0.04282387
1.994101448	0.029560137	0.028956208	0.038483989	0.041054068
1.997172004	0.029049066	0.028445847	0.036684489	0.039243909
2.000256033	0.028445847	0.027843464	0.034939479	0.037441264
2.003345587	0.027750864	0.027241916	0.033154576	0.035646071
2.006448726	0.027010773	0.026502691	0.031423665	0.033858267
2.009557455	0.026225806	0.025764723	0.02974613	0.032124554
2.012679883	0.025396208	0.024936004	0.028075051	0.03035116
2.015807966	0.024476287	0.024062958	0.026410377	0.028631363
2.018949863	0.023558311	0.023145853	0.024798038	0.026964559
2.022097481	0.022596519	0.022230682	0.023237477	0.025304128
2.025259031	0.021636853	0.021271823	0.021728158	0.023695883
2.028426367	0.020633758	0.020269569	0.020224067	0.022093572
2.031607753	0.019587538	0.019269623	0.018815863	0.020588217
2.034794994	0.01858916	0.018271975	0.017412209	0.019042684
2.037996405	0.017547849	0.017276612	0.016058141	0.017593071
2.041203739	0.016463918	0.01623844	0.014753209	0.016193358
2.044425363	0.015427684	0.015202743	0.013452187	0.014798142
2.04765298	0.014349026	0.014124643	0.012244383	0.013452187
2.050895011	0.013228266	0.013049212	0.01103993	0.01215505
2.054143104	0.01211039	0.011931797	0.009838807	0.010906307
2.057405735	0.010950844	0.010817249	0.008729611	0.009661145
2.0606745	0.009794385	0.009661145	0.007579044	0.008419543
2.063957928	0.008552402	0.008419543	0.006519681	0.007225636
2.067247563	0.007313961	0.00718148	0.005418919	0.006035002
2.070551988	0.005990967	0.005858889	0.004320939	0.004847623
2.073862694	0.004584201	0.00449643	0.003269485	0.003663482
2.077188318	0.003138232	0.003094489	0.002176919	0.002438884
2.080520297	0.00160987	0.001566281	0.001087096	0.00121773
2.083867324	0	0	0	0
2.087220782	0.000260655	0.000217202	8.68676E-05	8.68676E-05

Table A.9 Absorbance data Fig 4.8 (2 of 2)